



Materials Selection, Welding and Weld Monitoring

Final Report 278-T-02

for Project

Development of Optimized Welding Solutions for X100 Line Pipe Steel

Prepared for the

Design, Materials, and Construction Technical Committee of
Pipeline Research Council International, Inc.
Project MATH-1 Catalog No. L5XXXX

and

U.S. Department of Transportation
Pipeline and Hazardous Materials Safety Administration
Office of Pipeline Safety
DOT Project BAA DTPH56-07-000005

Prepared by
Radhika Panday
Joe Daniel

September 2011



Catalog No. L5XXXX

Materials Selection, Welding and Weld Monitoring

Final Report 278-T-02

for Project

Development of Optimized Welding Solutions for X100 Line Pipe Steel

Prepared for the

Design, Materials, and Construction Technical Committee of
Pipeline Research Council International, Inc.
Project MATH-1 Catalog No. L5XXXX

And

U.S. Department of Transportation
Pipeline and Hazardous Materials Safety Administration
Office of Pipeline Safety
DOT Project BAA DTPH56-07-000005

Prepared by

Radhika Panday
Joe Daniel

September 2011

Version	Date of Last Revision	Date of Uploading	Comments
4	21 March 2011	22 March 2011	Draft for TPC Review
5	17 May 2011	17 May 2011	Corrections made in Table 8 and 9.
6	18 August 2011	8 September 2011	Updated report with PHMSA comments

This report is furnished to Pipeline Research Council International, Inc. (PRCI) under the terms of PRCI contract] [278-PR- 348 - 074513], between PRCI and the MATH-1 contractors:

- Electricore (prime contractor),
- Center for Reliable Energy Systems, CANMET, NIST, and The Lincoln Electric Company (sub-contractors).

The contents of this report are published as received from the MATH-1 contractor and subcontractors. The opinions, findings, and conclusions expressed in the report are those of the authors and not necessarily those of PRCI, its member companies, or their representatives. Publication and dissemination of this report by PRCI should not be considered an endorsement by PRCI of the MATH-1 contractor and subcontractors, or the accuracy or validity of any opinions, findings, or conclusions expressed herein.

In publishing this report, PRCI and the MATH-1 contractors make no warranty or representation, expressed or implied, with respect to the accuracy, completeness, usefulness, or fitness for purpose of the information contained herein, or that the use of any information, method, process, or apparatus disclosed in this report may not infringe on privately owned rights. PRCI and the MATH-1 contractors assume no liability with respect to the use of, or for damages resulting from the use of, any information, method, process, or apparatus disclosed in this report. By accepting the report and utilizing it, you agree to waive any and all claims you may have, resulting from your voluntary use of the report, against PRCI and the MATH-1 contractors.

Pipeline Research Council International Catalog No. L5XXXX

PRCI Reports are Published by Technical Toolboxes, Inc.

3801 Kirby Drive, Suite 520
Houston, Texas 77098
Tel: 713-630-0505
Fax: 713-630-0560
Email: info@ttoolboxes.com

PROJECT PARTICIPANTS

PROJECT TEAM MEMBER	COMPANY AFFILIATION	PROJECT TEAM MEMBER	COMPANY AFFILIATION
Arti Bhatia	Alliance	Jim Costain	GE
Jennifer Klementis	Alliance	Gilmar Batista	Petrobras
Roger Haycraft	Boardwalk	Marcy Saturno de Menezes	Petrobras
David Horsley	BP	Dave Aguiar	PG&E
Mark Hudson	BP	Ken Lorang	PRCI
Ron Shockley	Chevron	Maslat Al-Waranbi	Saudi Aramco
Sam Mishael	Chevron	Paul Lee	SoCalGas
David Wilson	ConocoPhillips	Alan Lambeth	Spectra
Satish Kulkarni	El Paso	Robert Turner	Stupp
Art Meyer	Enbridge	Gilles Richard	TAMSA
Bill Forbes	Enbridge	Noe Mota Solis	TAMSA
Scott Ironside	Enbridge	Philippe Darcis	TAMSA
Sean Keane	Enbridge	Dave Taylor	TransCanada
Laurie Collins	Evraz	Joe Zhou	TransCanada
David de Miranda	Gassco	Jason Skow	TransGas
Adriaan den Herder	Gasunie	Ernesto Cisneros	Tuberia Laguna
Jeff Stetson	GE	Vivek Kashyap	Welsun
		Chris Brown	Williams

CORE RESEARCH TEAM	
RESEARCHER	COMPANY AFFILIATION
Yaoshan Chen	Center for Reliable Energy Systems
Yong-Yi Wang	Center for Reliable Energy Systems
Ming Liu	Center for Reliable Energy Systems
Dave Fink	Lincoln Electric Company
Marie Quintana	Lincoln Electric Company
Vaidyanath Rajan	Lincoln Electric Company
Joe Daniel	Lincoln Electric Company
Radhika Panday	Lincoln Electric Company
James Gianetto	CANMET Materials Technology Laboratory
John Bowker	CANMET Materials Technology Laboratory
Bill Tyson	CANMET Materials Technology Laboratory
Guowu Shen	CANMET Materials Technology Laboratory
Dong Park	CANMET Materials Technology Laboratory
Timothy Weeks	National Institute of Standards and Technology
Mark Richards	National Institute of Standards and Technology
Dave McColskey	National Institute of Standards and Technology
Enrico Lucon	National Institute of Standards and Technology
John Hammond	Consultant Metallurgist & Welding Engineer

This Page Intentionally Left Blank

FINAL REPORT STRUCTURE

Focus Area 1 - Update of Weld Design, Testing, and Assessment Procedures for High Strength Pipelines		
Report #	Description	Lead Authors
277-T-01	Background of Linepipe Specifications	CRES/CANMET
277-T-02	Background of All-Weld Metal Tensile Test Protocol	CANMET/Lincoln
277-T-03	Development of Procedure for Low-Constraint Toughness Testing Using a Single-Specimen Technique	CANMET/CRES
277-T-04	Summary of Publications: Single-Edge Notched Tension SE(T) Tests	CANMET
277-T-05	Small Scale Tensile, Charpy V-Notch, and Fracture Toughness Tests	CANMET/NIST
277-T-06	Small Scale Low Constraint Fracture Toughness Test Results	CANMET/NIST
277-T-07	Small Scale Low Constraint Fracture Toughness Test Discussion and Analysis	CANMET/NIST
277-T-08	Summary of Mechanical Properties	CANMET
277-T-09	Curved Wide Plate Tests	NIST/CRES
277-T-10	Weld Strength Mismatch Requirements	CRES/CANMET
277-T-11	Curved Wide Plate Test Results and Transferability of Test Specimens	CRES/CANMET
277-S-01	Summary Report 277 Weld Design, Testing, and Assessment Procedures for High Strength Pipelines	CRES

Focus Area 2 - Development of Optimized Welding Solutions for X100 Linepipe Steel		
Report #	Description	Lead Authors
278-T-01	State of The Art Review	Lincoln
278-T-02	Material Selection, Welding and Weld Monitoring	Lincoln/CANMET
278-T-03	Microstructure and Hardness Characterization of Girth Welds	CANMET/Lincoln
278-T-04	Microstructure and Properties of Simulated Weld Metals	CANMET/Lincoln
278-T-05	Microstructure and Properties of Simulated Heat Affected Zones	CANMET/Lincoln
278-T-06	Essential Welding Variables	Lincoln/CANMET
278-T-07	Thermal Model for Welding Simulations	CRES/CANMET
278-T-08	Microstructure Model for Welding Simulations	CRES/CANMET
278-T-09	Application to Other Processes	Lincoln/CANMET
278-S-01	Summary Report 278 Development of Optimized Welding Solutions for X100 Line Pipe Steel	Lincoln

EXECUTIVE SUMMARY

This is the second in the series of nine topical reports that detail the research contributing to the development of the optimized welding solutions for X100 line pipe steel. Two rounds of pipe welding were completed to understand the influence of the welding parameters on the weld metal and HAZ properties and microstructure. Thermal data was also obtained from these welds. This information was used to refine the thermal microstructural model with predictive capabilities. Essential welding variables were validated on flat plate experiments and recommendations for welding process control established. Ultimately, these recommendations were evaluated by pipeline welding contractors to assess its viability for field application.

It was observed that effective welding process control is important to achieve a sound and consistent weld. Of the numerous welding variables, True Heat Input showed a significant benefit as compared to the Average Heat Input for pulsed gas metal arc welding (GMAW-P) processes while the difference was negligible in case of constant voltage globular/shorting gas metal arc welding (GMAW) process.

TABLE OF CONTENTS

EXECUTIVE SUMMARY	vii
TABLE OF CONTENTS.....	viii
LIST OF FIGURES	ix
LIST OF TABLES.....	ix
ABSTRACT.....	1
1 BACKGROUND	2
2 TECHNICAL APPROACH.....	2
2.1 Test Welding	3
2.2 Weld Thermal Cycle Measurement Methods.....	5
2.3 Weld Process Monitoring Methods.....	10
2.4 Post Weld Evaluations	12
3 RESULTS AND DISCUSSIONS.....	13
3.1 Pipe Welds – First Round.....	13
3.2 Pipe Welds – Second Round	18
3.3 Plate Welds – Virtual Experiments	21
3.4 Pipe Welds – Third Round	22
3.5 Weld Monitoring - Measurement of Electrical Parameters	24
4 CONCLUSIONS & RECOMMENDATIONS.....	32
5 REFERENCES	34
6 APPENDIX 1.....	36

LIST OF FIGURES

Figure 1: Schematic of the CRC joint	4
Figure 2: Schematic of the compound joint used by Contractor B	5
Figure 3: Drilling fixture as positioned on pipe	6
Figure 4: Staggered weld passes used to facilitate thermocouple placement in specific fill passes	7
Figure 5: Elevation of drilling fixture during drilling	8
Figure 6: Sketch of drilling fixture after complete drilling to the required depth	8
Figure 7: Macrograph showing the placement of HAZ Thermocouple near Fill Pass 1	9
Figure 8: HAZ thermocouple location on pipe from First and Second Round pipe welding	9
Figure 9: Grounded thermocouple used in Round 1 pipe welding for HAZ	10
Figure 10: Implantable thermocouple used in Round 2 pipe welding and flat-plate welding for HAZ	10
Figure 11: True Energy™ Meter and Data Acquisition Unit	12
Figure 12b: Deposition of multiple internal root beads	15
Figure 12a: Internal root bead welding heads	15
Figure 13: Two-weld assembly with torch near 1:00	15
Figure 14: Detail view of P-GMAW X100 pipe	15
Figure 15: Fifteen Omega TJ K-type HAZ thermocouple placement	16
Figure 16: Time temperature profiles for 807K with grounded thermocouple located near the 4 th fill pass for Round 1	17
Figure 17: Comparison of the Average Heat Input with True Heat Input	18
Figure 18: Torch and thermocouple location along with the pass sequence for 1G staggered single and dual torch welds	19
Figure 19: Time Temperature Profile for 883J weld with Implantable thermocouple located near 1 st fill pass for Round 2	20
Figure 20: Data from Third Round Weld at Contractor B (Pipe 1 Side 2, Fill Pass 1)	27
Figure 21: Data from Third Round Weld at Contractor A (952-D Side 1, Fill Pass 1)	28

LIST OF TABLES

Table 1: Typical chemical composition, 914 mm dia. x 19 mm wall X100 base pipe for Round 1 and Round 2 pipe welding	4
Table 2: Typical chemical composition, 1067 mm x 14-15 mm wall X100 base pipe for Round 3 pipe welding	5
Table 3: Weld metal chemical compositions First Round Pipe Welds	15
Table 4: Weld Metal Chemical Compositions Second Round Pipe Welding	19
Table 5: Parameters for Third Round Pipe Welding	23
Table 6: Weld Metal Chemical Compositions Third Round Pipe Welds at Contractor A using 85% Ar - 15% CO ₂ Shielding Gas	23
Table 7: Weld Metal Chemical Composition Third Round Pipe Welds at Contractor B using 50% Ar - 50% CO ₂ Shielding Gas	24
Table 8: Measured Parameters for Figure 20	27
Table 9: Measured Parameters for Figure 21	29



TECHNICAL REPORT

No. (TH- 228)

FROM

**Consumable
Research &
Development**

**David C. Lincoln
Technology Center**

**The Lincoln Electric
Company**

September 29, 2011

**Radhika Panday
Joe Daniel**

Development of Optimized Welding Solutions for X100 Line Pipe Steel - Final Report – 278-T-02 – Materials Selection, Welding and Weld Monitoring

ABSTRACT

This is the second in the series of nine topical reports that detail the research contributing to the development of the optimized welding solutions for X100 line pipe steel. Two rounds of pipe welding were completed to understand the influence of the welding parameters on the weld metal and HAZ properties and microstructure. Thermal data was also obtained from these welds. This information was used to refine the thermal microstructural model with predictive capabilities. Essential welding variables were validated on flat plate experiments and recommendations for welding process control established. Ultimately, these recommendations were evaluated by pipeline welding contractors to assess its viability for field application.

It was observed that effective welding process control is important to achieve a sound and consistent weld. Of the numerous welding variables, True Heat Input showed a significant benefit as compared to the Average Heat Input for pulsed gas metal arc welding (GMAW-P) processes while the difference was negligible in case of constant voltage globular/shorting gas metal arc welding (GMAW) process.

KEYWORDS

GMAW-P, X100 pipe welding, weld metal, HAZ, thermocouples, True Power, True Heat Input, Average Heat Input, True Energy™

Note: Because many variables in design, fabrication, and service conditions affect the results obtained in applying this type of information, the testing and serviceability of a product or structure are the responsibility of the builder.

1 BACKGROUND

This investigation is part of a consolidated program of research co-funded by PRCI and PHMSA to advance the technology needed to support large-scale implementation of high strength steels in pipeline construction. A full description of the program, goals, and objectives is available from PRCI. The program is comprised of two complementary research programs:

- Project 277 - Update weld design, testing and assessment procedures for high strength steel pipelines, and
- Project 278 - Develop optimized welding solutions for X100 line pipe steel.

This report presents the details of the welding trials undertaken in the development of optimized welding solutions.

This is the second in a series of nine topical reports that detail the research leading to the development of optimized welding solutions. The ultimate goals of the project are welding solutions that ensure that increasing demands for strength, ductility, and toughness can be achieved consistently and confidently. This required a reassessment of essential welding variables in the context of the fundamental factors influencing the mechanical properties of high strength steel pipeline girth welds. Accordingly, for the range of weld and line pipe chemical compositions most likely to be employed, it was important to understand:

- The influence of welding process variables on thermal history in the weld region,
- The influence of weld thermal cycles on microstructure development in both the weld and heat affected zone (HAZ), and
- The influence of microstructure on mechanical properties.

Both experimental and numerical methods were used to accomplish this work. Results from initial welds were used to refine numerical analytical models. Numerical predictions were used to focus subsequent welding experiments, which led to further refinement of the models. In parallel, fundamental characterization of the weld and pipe materials led to an understanding of microstructures development under thermal conditions typical of the welding process.

Understanding the microstructure development for a range of chemical compositions established context for the weld properties. This led to a new reassessment of essential welding variable and recommendations for welding process control. Ultimately, these recommendations were evaluated by pipeline welding contractors to assess feasibility for field application.

2 TECHNICAL APPROACH

Significant research is been conducted on development of X100 line pipe and associated welding technology. Previous work [4-8, 11] suggested that control of welding parameters required greater precision than for lower strength pipe grades. This work was undertaken to gain a better understanding the effect of the essential welding variables on weld quality and properties. Numerous X100 girth pipe welds including 1G rolled single and dual torch welds, 5G single and

dual torch welds were completed to understand the effect of various welding variables on the weld and heat-affected zone (HAZ) properties.

One of the major goals of the project was the refinement of numerical models for predicting weld thermal cycles and properties. Ideally, such models would have the capability to accurately calculate the thermal cycles and final hardness in both weld metal and HAZ. The data generated from the full characterization of welding processes, such as welding parameters, temperature and thermal strain histories and post-welding micro-structural study from the experimental welds, was crucial for the verification of these models. In order to generate the necessary data for the model verification and the determination of essential variables, two rounds of girth welding on X100 pipe were undertaken at CRC-EVANS (CRC), followed by one round of flat-plate welding at Lincoln Electric Company. The final recommendations for the control of essential variables were assessed for field conditions under the third round of 5G girth welding on X100 pipe undertaken at CRC and Serimax.

2.1 Test Welding

Round 1 pipe welding involved making six X100 rolled girth welds utilizing single torch GMAW-P. This was basically a screening run for identifying the essential variables for X100 pipe welding and to produce a series of baseline welds. The welding was performed in 1G position by rolling the pipe to minimize the variations in the welding parameters with respect to the clock position. This also ensured the consistency of the deposited weld metal along the circumference of the pipe for the large number of mechanical test specimens for developing testing protocols under Project 277. The mechanical property results obtained from these welds correlated well with the essential welding variables which led to Round 2 pipe welding.

Round 2 included a total of seven GMAW-P welds. The three dual torch welds in 1G position were rolled to establish a baseline understanding of essential welding variables for the dual torch case and provide consistent weld metal for mechanical tests under Project 277. The spacing between the two torches was maintained at 120.65 mm (4.75 in.). The primary goal of the two 5G welds, one each single torch and dual torch, was to understand the effect of change in clock position on the welding parameters and hence the mechanical properties. The two staggered welds in 1G position, one each single and dual torch were completed to assess the effect of reheating by subsequent passes on microstructure formation and its correlation to the microhardness data. This is covered in detail in separate topical reports [12, 13].

The girth welding for the first two rounds was carried out on 914 mm (36 in.) diameter X100 pipes with a wall thickness of 19 mm (0.75 in.) supplied by TransCanada PipeLines. Pipe strings were fabricated using two 762 mm (30 in.) long pipe sections welded to a central 1524 mm (60 in.) long section. For single torch rolled welding trials, the torch was maintained at a clock position near 1:00, while the pipe rotated to simulate vertical down welding. This allowed nearly identical welding parameters to be achieved for the full circumference of the pipe. Similarly, for the dual torch rolled welds, the leading torch was positioned normal to the pipe near 12:30, while the trailing torch used a lead angle of several degrees and was positioned closer to 12:00.

The pipe ends were prepared using the standard CRC joint preparation, Figure 1, with a 5° bevel angle and 52° hot pass bevel angle. The offset distance was maintained at 2.5 mm (0.100 in.). The root pass bevel angle for the pipe was 37.5° while the land and root pass bevel depth were each 1.3 mm (0.050 in.). The root pass was deposited using ER48S-6 electrode conforming to AWS A5.18M while the remaining joint was filled in using a 1.0mm ER62S-G type electrode conforming to AWS A5.28M. This electrode, used in previous studies [9-11] over the last decade, was considered to be the best initial choice for achieving the required weld metal overmatch along with adequate ductility and low temperature toughness. The welding parameters selected for the CRC narrow groove were nominal for making a sound weld. The preheat and interpass temperature, which affect the weld cooling rates, was closely controlled between 100-125°C along with the nominal target heat input of 0.60-0.63 KJ/mm (15-16 kJ/in) to minimize the weld to weld and pass to pass variation and to get a consistent weld.

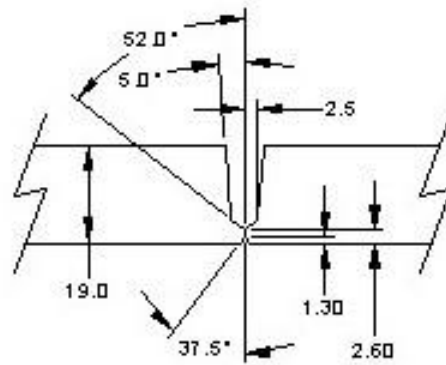


Figure 1: Schematic of the CRC joint

With a basis established for correlating welding thermal cycles and welding variables from First Round and Second Round of pipe welding, a series of flat plate experiments was conducted to gage the weld response to deliberate changes in welding parameters. Pipe remaining from First and Second Rounds was cut and flattened for conducting flat plate welds. These were prepared using the CRC joint without the ID root pass bevel, and with offsets of 2.3 mm (0.090 in.), 2.5 mm (0.100 in.) 2.8 mm (0.110 in.) A schematic of the CRC compound joint is shown Figure 1 while the typical chemical composition of the pipe is given in Table 1. It is evident from the pipe chemistry that it is not the latest generation pipe due to lower %Nb content. The information obtained from flat plate welding was further used to refine the thermal model and details are available under separate topical reports [15, 16].

Table 1: Typical chemical composition, 914 mm dia. x 19 mm wall X100 base pipe for Round 1 and Round 2 pipe welding

%C	%Mn	%Si	%S	%P	%Ni	%Cr	%Mo
0.07	1.83	0.11	0.005	0.005	0.52	0.03	0.27
%Cu	%Al	%Nb	%V	%Ti	%B	%N	
0.303	0.042	0.027	0.002	0.009	0.0001	0.004	

Once all the essential welding variables were identified and validated, it was necessary to understand the viability of implementing these controls under fabrication conditions. Hence, the Third Round X100 girth welding were completed by two contractors, Contractor A and Contractor B, using pipes from two different mills, Table 2, supplied by TransCanada PipeLines. These pipes were 1067 mm (42 in.) in diameter with a 14-15 mm (0.55-0.59 in.) nominal wall thickness. Both single and dual torch girth welds were made. Both the contractors used their own power sources (Contractor A used Fronius 3200 while Contractor B used Saturnax 05), weld schedules, gas mixtures and torch gap configurations. For the welding completed at Contractor A, the pipe ends were prepared using the standard CRC joint shown in Figure 1. Contractor B used their standard joint, with a 4° bevel angle and an offset distance of 2.4 mm (0.100 in.). The radius of the joint was equal to the offset. The land was maintained between 1.80 to 1.85 mm (0.070 to 0.073 in.) A schematic of the compound joint used by Contractor B is shown in Figure 2, while the typical chemical composition of the pipes is given in Table 2.

Table 2: Typical chemical composition, 1067 mm x 14-15 mm wall X100 base pipe for Round 3 pipe welding

Pipe	%C	%Mn	%Si	%S	%P	%Ni	%Cr	%Mo	%Cu	%Al	%Nb	%Ti
A	0.06	1.90	0.32	0.001	0.012	0.23	0.23	0.23	0.23	0.038	0.043	0.017
B	0.05	1.97	0.18	*	0.008	0.45	0.48	0.10	0.48	0.012	0.021	0.012

* Below the detection limit of the instrument

All the welds, including pipe and flat plate welds were thoroughly monitored for thermal data, in-process welding parameters such as voltage, current, wire feed speed, travel speed, preheat and interpass temperature and True Power. This data was then utilized to calculate the Average Heat Input and True Heat Input values. The details on monitoring the thermal data and True Power will be discussed later.

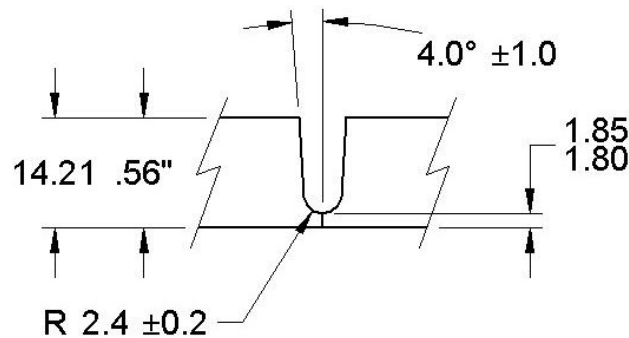


Figure 2: Schematic of the compound joint used by Contractor B

2.2 Weld Thermal Cycle Measurement Methods

The first step towards generation of thermal data for numerical model refinement was to develop a reliable means to measure the thermal histories in the weld metal and HAZ. K-type thermocouples were accurately positioned 1 to 2 mm from the fusion boundary for HAZ measurements, while S-type thermocouples were used for the weld metal thermal measurements.

For First Round and Second Round of welding, three HAZ thermocouples for each fill pass were embedded in the holes drilled from the ID of the pipe. Three thermocouples for each fill pass built in the required redundancy to offset occasional failure of the thermocouple due to variation in placement relative to the fusion boundary.

2.2.1 Drilling Method

A drilling fixture was designed for accurate positioning of the drilled holes for thermocouple placement, Figure 3. These holes are required to be drilled prior to welding the two pipe joints together. The drilling fixture is clamped onto the ID of the pipe or inside surface of the flat plate perpendicular to the joint face using a C-clamp such that the drill is located at a 45° angle from the surface of the pipe. Drill size was slightly larger than the thermocouples being used and was varied for the two different K-type thermocouple used. The externally grounded thermocouples required a 1.59 mm (1/16 in.) diameter drill while the ceramic sleeve thermocouples used a 1.70 mm (0.067 in.) diameter (#51) drill.

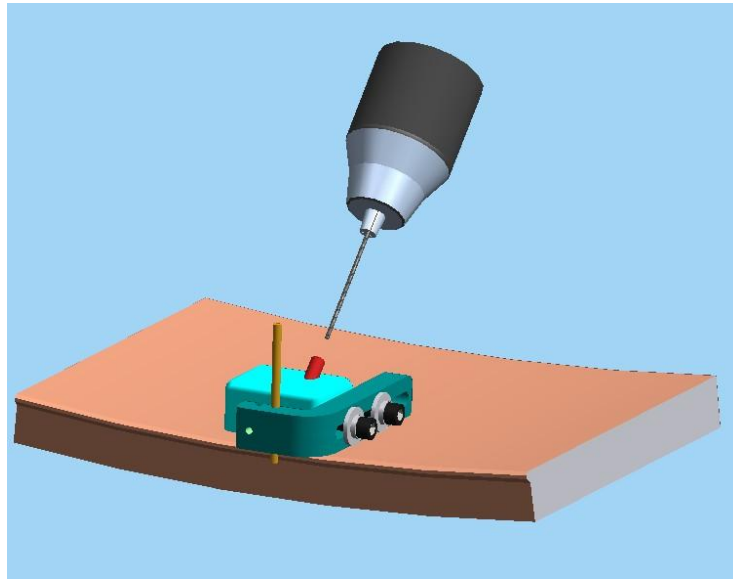


Figure 3: Drilling fixture as positioned on pipe

To determine proper placement of the drilling fixture a series of trial plate welds were made using joint configuration and weld parameters identical to the first round pipe welds. Welds were staggered with successive passes, each stopping approximately 50 mm short of the previous pass. A section from each pass was cut and etched to reveal the HAZ and fusion boundaries as shown in Figure 4. Trials were made to determine the fixture position and approximate depth of hole needed to facilitate thermocouple placement in the coarse grained HAZ adjacent specific fill passes, 1 to 2 mm from the fusion boundary. The drilling fixture was placed on the ID surface of a section with the drill bit inserted through the guide bushing and against the etched face. With the jaws of the drill chuck contacting the upper end of the guide bushing, the stick out of the drill bit was adjusted to the desired depth and the chuck tightened.

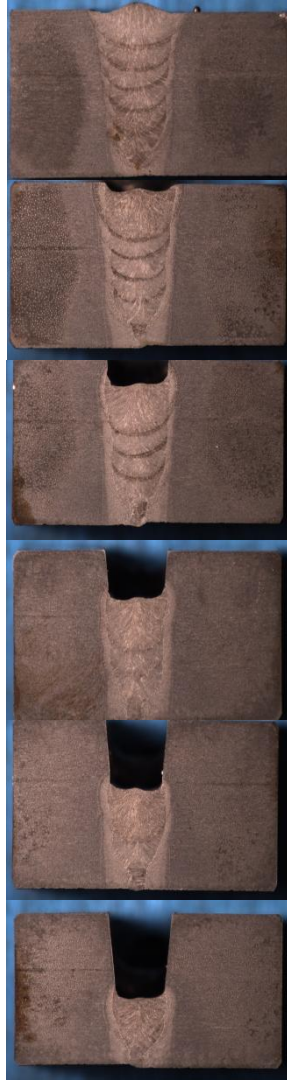


Figure 4: Staggered weld passes used to facilitate thermocouple placement in specific fill passes

Test holes for thermocouple placement were then drilled in an un-welded test plate with a machined joint preparation. With the fixture base on the ID surface and the flat on the gauge pin contacting the joint root face, the drill was inserted in the guide bushing. The gauge pin arm was adjusted in the slide so that the drill bit was at the proper distance from the joint wall for the thermocouple location of interest. The position was locked in by tightening the two screws on the fixture base and clamping the fixture onto the ID surface at the guide bushing. See Figures 3, 5 and 6. Drilling proceeded until the bit started to deform the joint wall and was stopped before the bit came through the joint surface, Figure 5. Occasionally, it was necessary to remove the fixture and finish drilling with light pressure controlled by hand until the surface deformation appeared on the joint wall. The test weld was assembled and the ID root pass on the pipe completed before thermocouples were inserted into each hole targeting a specific HAZ location. While care was taken to cover the holes during root pass welding to prevent spatter from clogging the holes, it was sometimes necessary to lightly drill out any debris prior to inserting the thermocouples. The weld was completed in the staggered manner previously described. This

drilling technique was found to be reliable and repeatable after a series of staggered plate welds were sectioned and analyzed to confirm that the drilled holes were right at the target location near the fusion boundary. An example of the thermocouple placement for HAZ cooling rate measurements is shown in Figure 7.

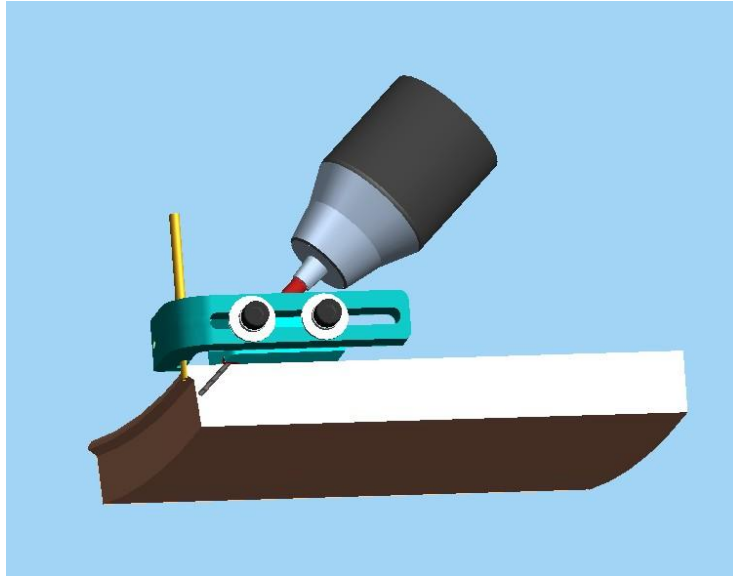


Figure 5: Elevation of drilling fixture during drilling

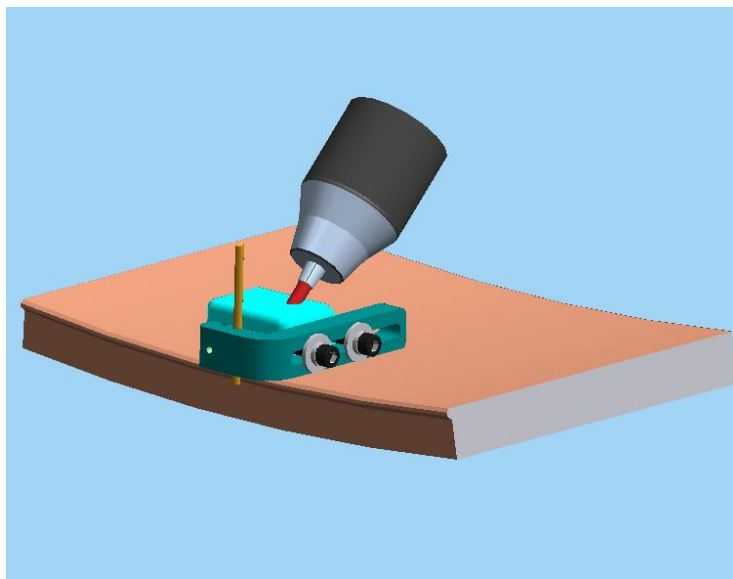


Figure 6: Sketch of drilling fixture after complete drilling to the required depth

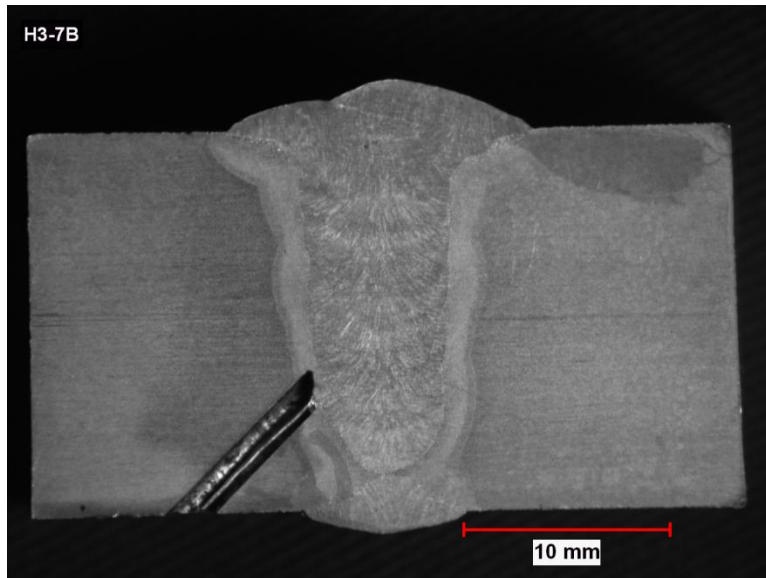


Figure 7: Macrograph showing the placement of HAZ Thermocouple near Fill Pass 1

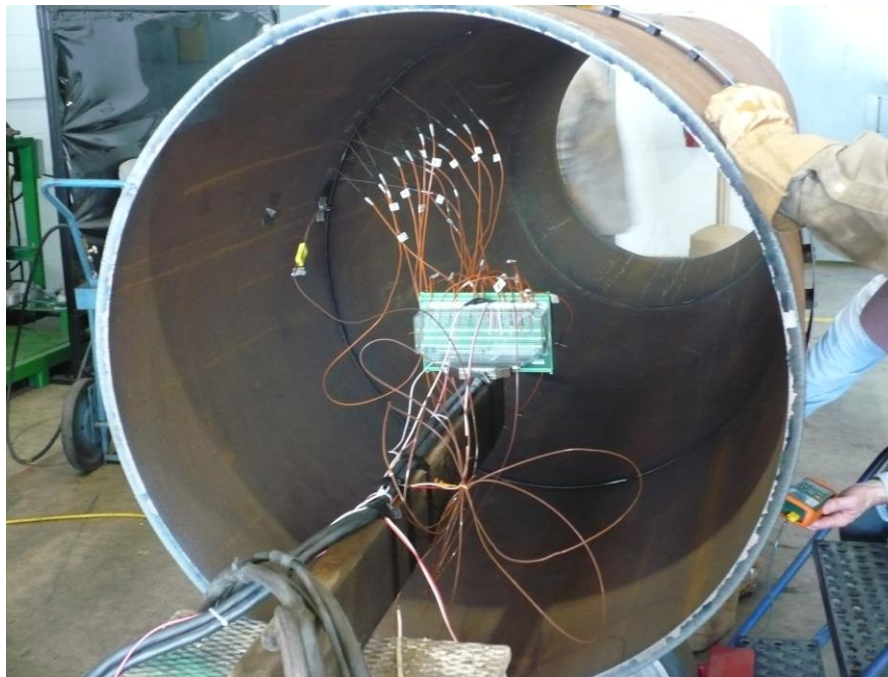


Figure 8: HAZ thermocouple location on pipe from First and Second Round pipe welding

2.2.2 Thermocouples

The goal for use of both types of thermocouples was the measurement of the HAZ thermal profiles. The thermocouples were placed at an angle between 30° to 75° from the torch position as shown in Figure 8.

As mentioned earlier, different K-type thermocouples were used for First and Second Round pipe welding. The Omega TJ-36-CAXL-116G-6 thermocouples shown in Figure 9 were used for First Round pipe welding. These thermocouples have a diameter of 1.59 mm (1/16 in.) with the K-type wires grounded at the tip of the Inconel sheath which surrounds the wires. These thermocouples were just inserted into the drilled holes making sure that the tip of the thermocouple made a firm contact with the base of the drilled hole near HAZ. K-type HAZ thermocouples used for Second Round pipe welding and flat plate welding were ceramic covered “implantable” thermocouples, shown in Figure 10, designed using Omega TT-K-30 duplex insulated wires and 1.59 mm (1/16 in.) diameter two-hole ceramic insulating sleeve. The 0.254 mm (0.010 in.) thermocouple wires were passed through a 7.94 mm (5/16 in.) length of heat shrink tubing and through the insulating sleeve. The wires were joined at the pointed end using a Rofin-Bassel Laser welder. The laser welded exposed junction on these thermocouples was welded to the bottom of the holes with a capacitor discharge welder to ensure complete contact.

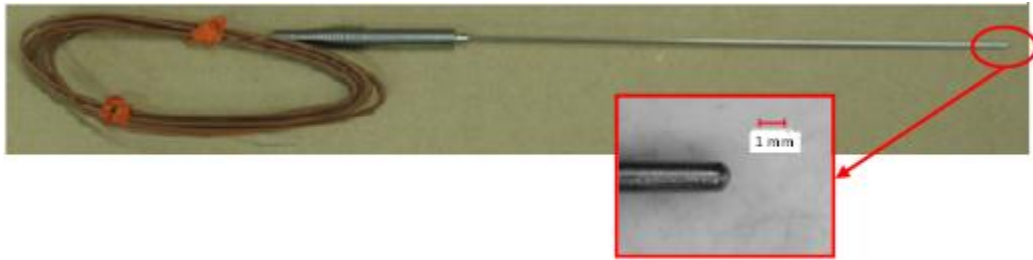


Figure 9: Grounded thermocouple used in Round 1 pipe welding for HAZ

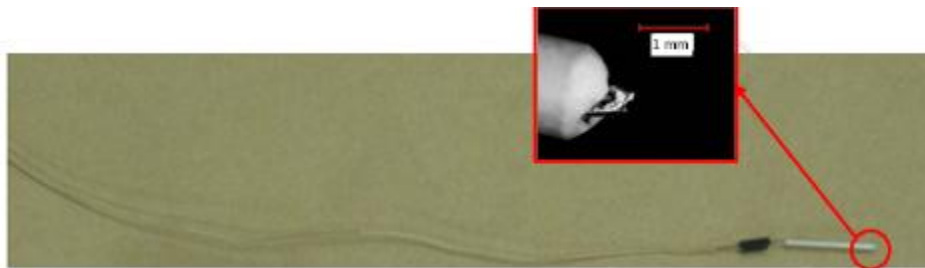


Figure 10: Implantable thermocouple used in Round 2 pipe welding and flat-plate welding for HAZ

S-type thermocouples, rated for temperatures up to 1700°C, were used for plunging into the weld metal for hot, fill and cap passes for obtaining the weld metal thermal data. The 0.76 mm (0.03 in.) S-type bare thermocouple wires were inserted into a suitable ceramic sleeve and TIG welded at the junction. All the thermocouples were connected to a National Instruments Isothermal terminal block which was connected through its chassis to a laptop computer running a NI Labview Signal Express program. The thermal data was collected from each thermocouple at a sampling rate of 1KHz. Refer Appendix 1 for detailed connections. The thermal response from the K-type HAZ thermocouples and S-type weld metal thermocouples will be discussed later.

2.3 Weld Process Monitoring Methods

Accurate and complete data collection during the welding operation is a core requirement of this project. Correlation of mechanical properties and the ultimate determination of the essential welding variables, a fundamental task of this project, cannot be accomplished without the

electrical welding data described herein. On the surface, the required electrical welding data (voltage, amperage, and heat input) may not seem to be anything out of the ordinary but special considerations needs to be followed. They are important because the data needs to accurately reflect the conditions at the arc.

In addition to thermal data monitoring, in-process monitoring of welding operations included voltage, current, travel speed, wire feed speed, preheat temperatures, and interpass temperatures. These were used to calculate Average Power, True Power, Average Heat Input and True Heat Input

1. Voltage Measurement (and Welding Voltage Control)

Voltage measurement points were located as close to the arc as possible in order to avoid measurement errors due to voltage drop in cable and connections. In general:

- Positive voltage measurement points were located where the welding torch and the electrode cable are connected. This is typically a brass connection block on the wire feeder.
- Negative, or ground, voltage measurement points were located directly on the work piece.

2. Current Measurement and Control

The amperage measurement is more straightforward because the current can be measured on the electrode or work cable without special considerations. However, the measurement device for the amperage must have an adequate frequency range as described in the next section.

3. Heat Input Calculation

The pulsed gas metal arc welding (GMAW-P) waveforms used on this project are complex welding waveforms that are not represented accurately by a conventional heat input calculation as in Equation 1. The product of average voltage and average amperage, in this case, does not accurately represent the conditions in a complex waveform, even though this heat input is an essential welding variable identified by many fabrication codes.

$$\text{Heat Input (J/in.)} = \frac{\text{Voltage} * \text{Amperage} * 60}{\text{Travel Speed (in./min.)}}$$

Equation 1: Average Heat Input Calculation

An accurate calculation of heat input can only be determined by the ratio of the True Energy by the travel speed. The fundamental change with the complex waveform calculation is to include True Energy, or True Power, that must be found from instantaneous power measurements as in Equation 2.

$$\text{Heat Input (J/in.)} = \frac{\text{True Energy (J)}}{\text{Length of Weld (in.)}}$$

or

$$\text{Heat Input (J/in.)} = \frac{\text{True Power (W or J/s)} * \text{Time(s)}}{\text{Length of Weld (in.)}}$$

Equation 2: True Heat Input Calculation

4. True Power

Instantaneous power measurements at a rate of at least 5 kHz to 10 kHz will create an accurate representation of the conditions occurring in a complex welding waveform.

The Lincoln Electric data acquisition system used for high frequency (40 kHz) voltage and current measurements is shown in Figure 11 and was employed for determination of True Heat Input.



Figure 11: True Energy™ Meter and Data Acquisition Unit

2.4 Post Weld Evaluations

All the welded pipe joints and the flat plate welds were examined to help explain the effects of essential welding variables on weld properties and the techniques/test methods are described below:

2.4.1 NDT

Radiographic testing (X-Ray) and Automatic Ultrasonic Testing (AUT) were performed on all the single and dual torch 1G welds from First and Second Round and the 5G welds from Second Round for verification of weld soundness. Only radiographic testing was performed on the flat plate and Third Round welds due to the time and cost involved for AUT. The X-rays were done in-house at CRC while the AUT was completed by a contractor, UT Quality Inc. The results from X-ray and AUT analysis were used to generate a defect map for each weld. A defect map helped segregate the defective weld areas from the sound ones with respect to the clock position.

This allowed for efficient positioning and sectioning of the weld metal and HAZ for chemical analysis, hardness mapping, round bar and strip tensile, Charpy toughness, crack tip opening displacements (CTOD), single edged notched tensile (S(E)NT), single edged notched bending (S(E)NB) and curved wide plate specimens.

2.4.2 Chemical Analysis

Chemical analysis was performed on each weld on samples from three different clock positions, 12:00, 3:00 and 6:00. The weld metal chemistry was used to calculate the carbon equivalents and transformation start temperatures along with the weld metal hardenability. A 19.05 mm (0.75 in.) thick macro was cut and sectioned longitudinal to the weld. The exposed all-weld metal side was surface ground and analyzed for all the relevant elements using an OBLF OSG 750 Optical Emission Spectroscopy. The weld metal was further cut into 5 mm x 5 mm specimens weighing about 2 grams for LECO carbon and sulfur C & S using CS-600 and nitrogen and oxygen N & O using TC-436 DR analysis.

2.4.3 Micro Hardness Mapping

Micro hardness maps were generated on each weld from three different clock positions, 12:00, 3:00, and 6:00. The hardness information obtained from these maps was used to correlate the microstructure and the weld metal properties. 6.35-12.70 mm (0.25-0.50 in.) thick macro samples were machined from the pipe and mounted in epoxy resin. The specimens were further ground, and then polished using a series of diamond suspensions and a final polish with a 1 μ m colloidal silica suspension followed by etching with 3% Nital solution. A macro photo of each polished specimen was taken under an optical microscope before and after the microhardness indentation. Micro hardness mapping was done using an automatic Clemex Matsuzawa diamond pyramid indenter with a 300 gram force. At least 3000 indents were made on each specimen (50 x 60 grid) with a constant spacing of 300 μ m between each indents. Detailed procedures are included in the topical report 278-T-03 on weld microstructures [12]. Post-test data processing was used to create individual color maps with hardness interval fixed at ten points per color code.

2.4.4 Metallography

As with chemical analysis and micro hardness mapping, transverse metallographic specimens were sectioned from each weld from 3 different clock positions, 12:00, 3:00, and 6:00. Detailed information on the sample preparation and analysis of the microstructures are provided in topical report 278-T-03 [12].

3 RESULTS AND DISCUSSIONS

3.1 Pipe Welds – First Round

First round of welding involved making preliminary set-in trial welds to establish the nominal welding conditions prior to the actual pipe welding. Six X100 rolled girth welds were made utilizing the single torch on the pipe and 1.0 mm ER62S-G type welding consumable conforming

to AWS A5.28M 85% Ar - 15% CO₂ shielding gas. These welds were made following deposition of the internal root passes in the 5G position with ER48S-6 type electrode and 75% Ar - 25% CO₂ shielding gas and Fronius 3200 power source. The hot pass, five fill passes and cap pass were made from the outside with a single torch positioned near 1:00, while the pipe was rotated to achieve consistent weld metal as shown in Figures 12-14. Fig. 12a displays the internal root bead welding head assembly while Fig. 12b shows the root bead being welded on the ID of the pipe (three arcs visible around the pipe). The detailed weld chemistry for the six welds taken from near 1:00 is shown in Table 3. As mentioned earlier, all the welds were closely controlled and monitored to record the weld thermal history and weld data, like True Power, Average Heat Input, volts, current, and travel speed. The minimum preheat temperature was strictly maintained at 100°C while the maximum interpass temperature was not allowed to exceed 125°C. Further experimental assessment of weld thermal cycles was carried out on two of the six welds. Fifteen Omega TJ grounded thermocouples were inserted into pre-drilled holes between 30° to 75° from the torch position. Three thermocouples were inserted to each of five depths coinciding with fill passes 1 through 5. Three thermocouples for each fill pass built-in the required redundancy to offset the occasional failure of a thermocouple due to variation in the placement location or weld oscillation as shown in Figure 15. An S-type thermocouple was also plunged into the weld metal for the hot, fill and cap pass. Data recording began at the arc start. The thermocouples encountered the arc early in the weld cycle and data was recorded throughout the cycle to measure cooling rates until the thermocouple readings dropped to below 140°C.



Figure 12a: Internal root bead welding heads



Figure 12b: Deposition of multiple internal root beads



Figure 13: Two-weld assembly with torch near 1:00



Figure 14: Detail view of P-GMAW X100 pipe

Table 3: Weld metal chemical compositions First Round Pipe Welds

ID	%C	%Mn	%Si	%Ti	%Cr	%Mo	%Ni	%N	%O	%S	%P	%Al	%Cu
Weld-807F	0.114	1.38	0.54	0.032	0.05	0.35	0.95	0.008	0.024	0.012	0.013	0.006	0.130
Weld-807G	0.103	1.39	0.56	0.035	0.05	0.35	0.95	0.014	0.023	0.012	0.013	0.007	0.138
Weld-807H	0.105	1.39	0.56	0.035	0.05	0.35	0.95	0.009	0.024	0.012	0.012	0.006	0.140
Weld- 807I	0.109	1.39	0.55	0.034	0.05	0.35	0.95	0.009	0.022	0.012	0.013	0.008	0.139
Weld-807J	0.097	1.39	0.58	0.038	0.05	0.35	0.96	0.007	0.022	0.011	0.013	0.005	0.134
Weld-807K	0.104	1.40	0.56	0.035	0.05	0.35	0.96	0.010	0.022	0.012	0.012	0.006	0.140

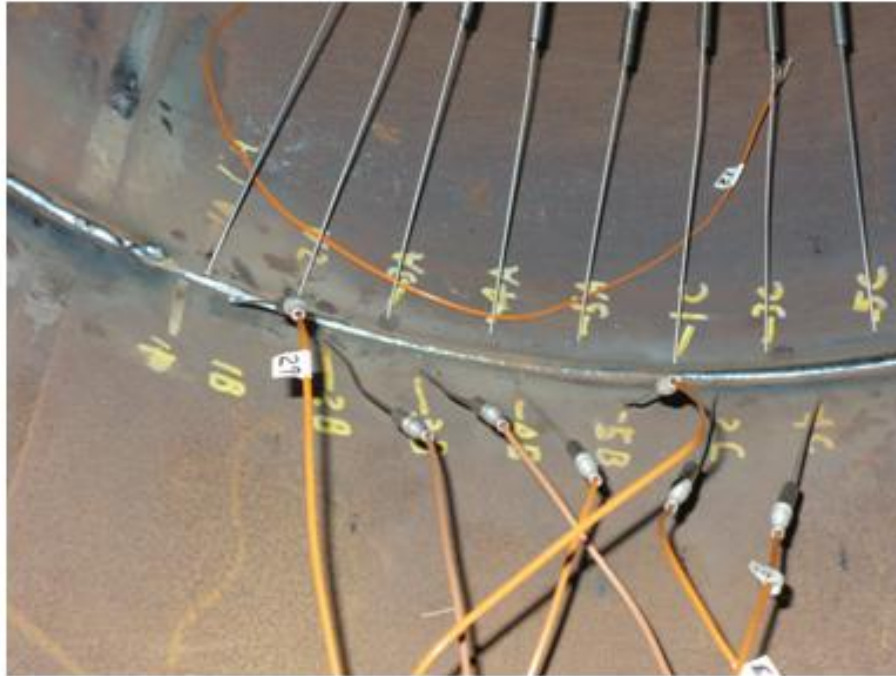


Figure 15: Fifteen Omega TJ K-type HAZ thermocouple placement

The six 1G rolled welds from 807F through 807K are very similar in weld metal chemical composition validating the fact that the welding parameters were maintained constant throughout the pipe welding.

Most of the K-type HAZ thermocouple survived (80%) the welding arc and meaningful thermal data was obtained. Figure 16 shows the HAZ thermal profile for Omega TJ thermocouple located near the fourth fill pass for 807K weld. The highest peak temperature reached is 1050°C with most of the thermocouples while with some the peak temperature recorded was less than 500°C. Since the K-type thermocouples are rated to measure maximum temperature up to 1300°C, it is believed that in the cases where the recorded peak temperatures were less than 500°C, these thermocouples were not placed close enough to the HAZ and hence did not record the peak temperatures expected. The weld plunging experiments with S-type thermocouples were only moderately successful and meaningful data could be obtained from two or three thermocouples out of seven plunges for each of these welds.

The Average Heat Input was calculated from the data gathered from the CRC welding system for voltage, current and travel speed, while the True Power was calculated using the instantaneous data collected from the True Energy™ meter. It should be noted that, for each of the pipe welds, the nominal Average Heat Inputs for the hot pass, fill passes 1 thru 4, fill pass 5, and cap pass were 0.21 kJ/mm (5.3 kJ/in), 0.59 kJ/mm (15 kJ/in), 0.65 kJ/mm (16.5 kJ/in) and 0.50 kJ/mm (12.7 kJ/in), respectively. The corresponding nominal True Heat Inputs were 0.24 kJ/mm (6.1 kJ/in), 0.68 kJ/mm (17.2 kJ/in), 0.75 kJ/mm (19 kJ/in) and 0.61 kJ/mm (15.6 kJ/in). (See Figures 17a and 17b) Thus, the overall average of the True Heat Input for all welds was 15-23% higher than the corresponding Average Heat Inputs.

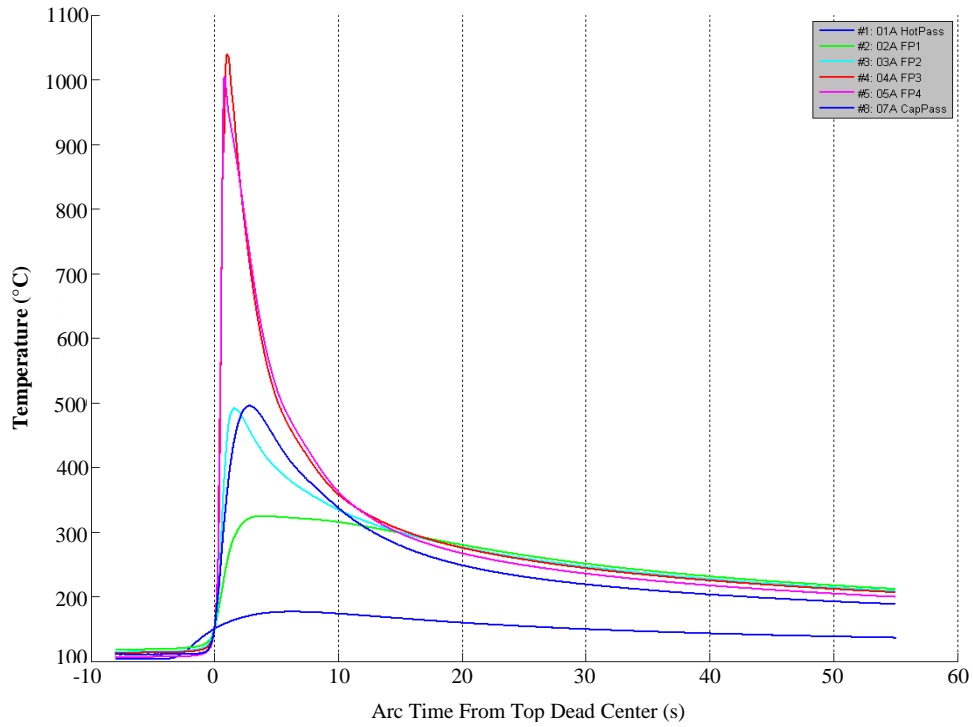
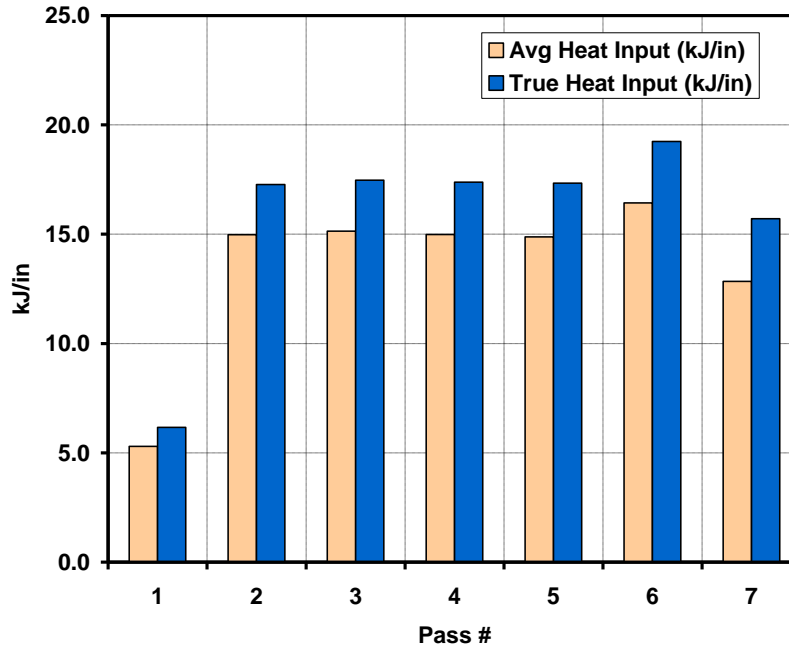


Figure 16: Time temperature profiles for 807K with grounded thermocouple located near the 4th fill pass for Round 1

(a) Pipe Weld 807K



(b) Pipe Weld 807G

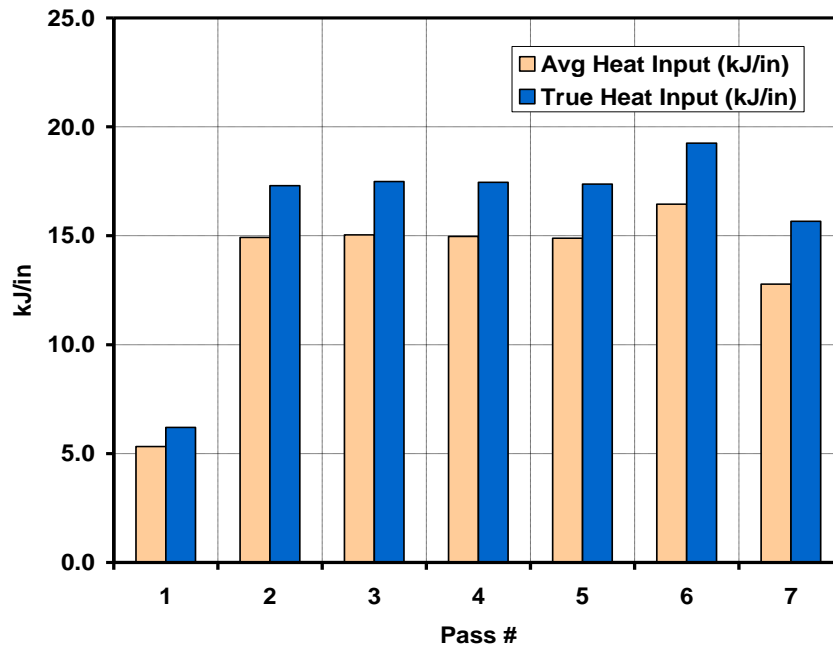


Figure 17: Comparison of the Average Heat Input with True Heat Input

3.2 Pipe Welds – Second Round

The second round of welding to produce seven girth welds was completed at CRC. Pipe used was from the same heat as that in the first round of welding. Three dual torch rolled X100 welds, one dual torch staggered rolled weld, one single torch staggered rolled weld, one dual torch 5G weld and one single torch 5G weld were completed on X100 pipe with a 1.0 mm ER62S-G type welding consumable conforming to AWS A5.28M and 85% Ar – 15% CO₂ shielding gas. The internal root pass for all the seven welds was made in the 5G position with ER48S-6 type electrode and 75%Ar-25%CO₂ shielding gas and a Fronius 3200 power source. For the dual torch rolled welds 883D through 883F, the hot pass, first, third, and fifth fill passes and capping pass were made using the lead torch positioned normal at 12:30 while the second and fourth fill passes were made by the trail torch which was positioned 19.05 mm (4.75 in.) behind the lead torch. For the 1G single torch staggered weld 883I, the hot pass, five fill passes and cap pass were made from the outside with the torch positioned near 1:00 while the pipe was rotated. The torch location for 1G dual torch staggered weld 883J was similar to the 1G dual torch welds mentioned earlier. The single torch and dual torch staggered welds had three K-type implantable HAZ thermocouples each embedded at depths of approximately 7 mm, 9.8 mm and 12.6 mm from the pipe ID surface to represent the top of the first, second and third fill region approximately. These thermocouples were positioned between 30° to 75° from the lead torch. The thermocouple placement location and the pass sequence for the 1G staggered welds are shown in Figure 18. The end point for each pass is indicated by a black marker in conjunction with the respective pass number. Additionally, for the single torch staggered weld, S-type thermocouples were plunged for each pass soon after the welding was initiated. For the dual torch staggered weld, the S-type thermocouple was plunged in the puddle of the trailing/second torch.

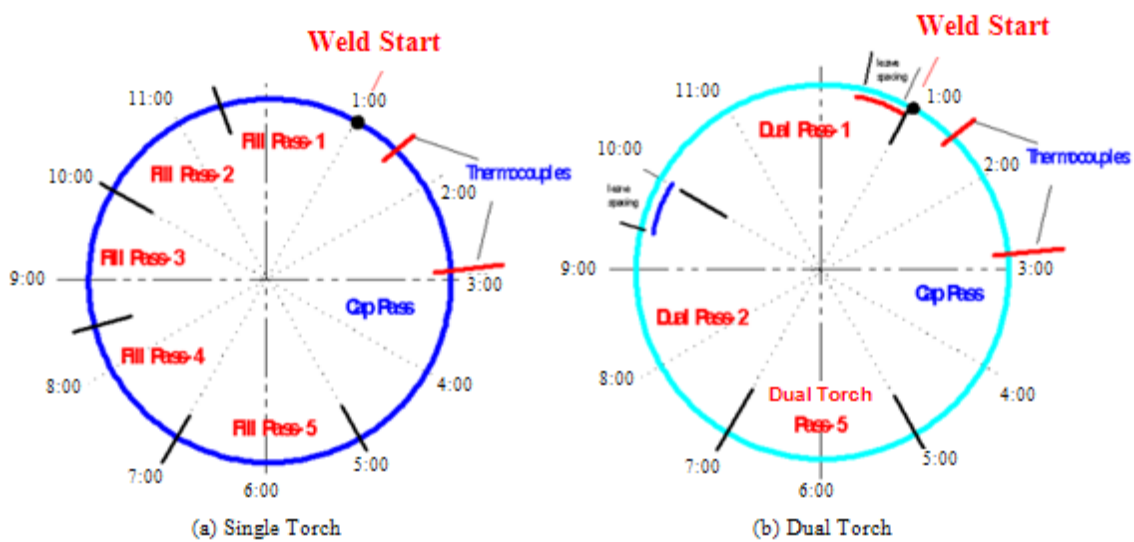


Figure 18: Torch and thermocouple location along with the pass sequence for 1G staggered single and dual torch welds

The two 5G welds, single torch (883G) and dual torch (883H) had four K-type HAZ thermocouples each embedded approximately at the 2:00 – 3:00 position and 5:00 – 6:00 position. As with the first round of welding, all the welds were closely controlled and monitored to record the weld thermal history and weld data, like voltage, current, travel speed and True Power. The minimum preheat temperature was strictly maintained at 100°C while the maximum interpass temperature was not allowed to exceed 125°C. The detailed weld compositions for the six welds taken from near 12:00 position are shown in Table 4.

Table 4: Weld Metal Chemical Compositions Second Round Pipe Welding

Pipe ID	%C	%Mn	%Si	%Ti	%Cr	%Mo	%Ni	%N	%O	%S	%P	%Al	%Cu
Weld 883D	0.112	1.48	0.56	0.038	0.07	0.36	0.99	0.004	0.032	0.011	0.014	0.005	0.143
Weld 883E	0.113	1.44	0.55	0.037	0.06	0.35	0.96	0.004	0.031	0.011	0.014	0.006	0.137
Weld 883F	0.113	1.43	0.57	0.036	0.06	0.35	0.98	0.004	0.025	0.011	0.014	0.006	0.130
Weld 883G	0.110	1.42	0.56	0.038	0.05	0.35	0.96	0.004	0.028	0.010	0.014	0.008	0.137
Weld 883H	0.107	1.43	0.55	0.035	0.07	0.37	0.99	0.004	0.031	0.010	0.014	0.004	0.137
Weld 883I	0.111	1.44	0.59	0.039	0.06	0.35	0.96	0.004	0.030	0.011	0.014	0.005	0.132
Weld 883J	0.113	1.45	0.57	0.037	0.05	0.35	0.95	0.004	0.033	0.011	0.014	0.008	0.136

The weld metal chemical composition for all the welds made under Second Round irrespective of the welding position or torch configuration is almost the same and very comparable to the First Round welds validating that with proper control of the welding variables consistent weld metal composition can be obtained. The little variation seen in the %Mn analysis between the

First Round welds and Second Round welds is representative of the variation between the heats of steel used to manufacture the welding consumable.

It was speculated that the peak temperatures from the thermal data for the First Round did not reach the temperatures expected due to the design of the grounded thermocouple which may have restricted its proximity to the coarse grained HAZ which is the desired location for thermocouple placement. Hence, for the Second Round welding, “implantable” thermocouples with exposed junctions were spot welded onto the base of the pre-drilled holes adjacent to the coarse grained HAZ. The objective was to get the junction closer to the HAZ location of interest. Figure 19 shows the thermal response of implantable thermocouple located near first fill pass for weld 883J.

As seen from the graph in Figure 19 the maximum temperature reached with these implantable thermocouples was a little over 1150°C and only slightly higher than that obtained with the Omega TJ grounded thermocouples from First Round.

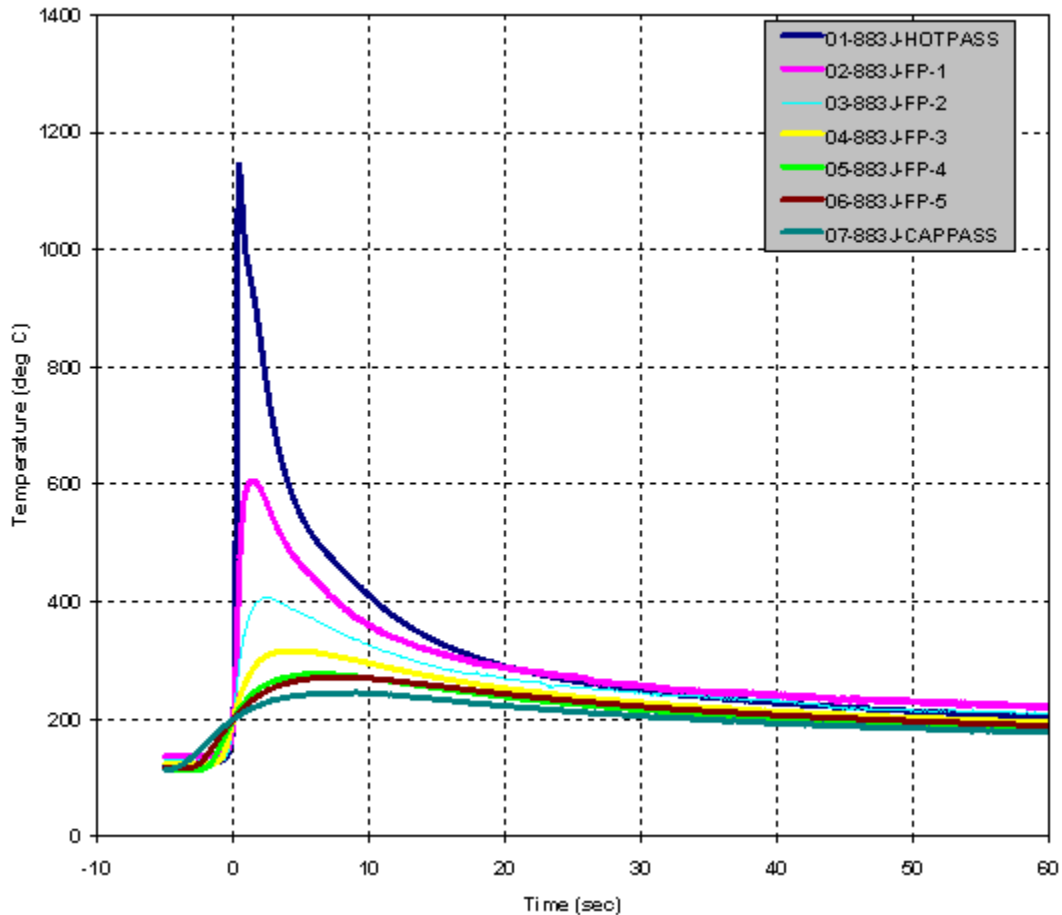


Figure 19: Time Temperature Profile for 883J weld with Implantable thermocouple located near 1st fill pass for Round 2

In spite of the care and effort involved in making and positioning these implantable thermocouples, only 50% of the implantable K-type HAZ thermocouples survived the welding

arc to give any meaningful thermal data. The survival rate for the S-type plunge thermocouples was also nearly 50%. This data was sufficient to obtain the necessary information about the cooling rates for integration with the thermal model.

The Average Heat Input was calculated from the data gathered from the CRC welding power source for voltage, current and travel speed while the True Energy Heat Input was calculated using the instantaneous data collected from the True Energy meter. Since only one True Power meter was available, for dual torch welds, only data from either the lead or trail torch could be recorded at given time. In this round of welding also, the True Heat Input results were 15-18 % higher than the calculated Average Heat Input values.

3.3 Plate Welds – Virtual Experiments

The thermal and microstructure models relied upon data generated from the first and second rounds of pipe welds and the microstructure characterizations from the Topical reports [12, 13]. The numerical tool developed from these models correlated True Heat Input with hardness. The ability to predict shifts in hardness with variation in True Heat Input allowed engineers to focus on the welding process variables most likely to influence weld properties by running a series of numerical simulations under Topical report 278-T-07 and 278-T-08 [15, 16]. This identified the welding process variable to be used in this next phase of experiments. Plate welds rather than pipe welds were conducted to reduce the cycle time per test and conserve X100 material that was in short supply. Twenty-nine experimental plate welds were made on pipe material that was obtained from the pipe pieces remaining from the first and second round of welding. These pieces were flattened into plate and a groove similar to that used in the first and second round of welding (CRC joint without the back bevel and root bead) was employed for these flat plate welds. The variables studied in the testing include:

- Preheat/Interpass Temperatures: 27°C, 100°C, 180°C
- Consumable Composition Pcm: 0.22, 0.28, 0.33
- Two different proprietary pulse waveforms resulting in the following ranges for the True Heat Input
 - True Heat Input: 0.47-0.55 kJ/mm (12-14 kJ/in), 0.83-0.91 kJ/mm (21-23 kJ/in)
 - True Heat Input/ Wire Feed Speed (WFS)/ Travel Speed (TS) ratio: 0.62 – 0.89
- Groove Offset Distance: 2.3 mm (0.090 in.), 2.5 mm (0.100 in.), 2.8 mm (0.110 in.)
- Torch Configuration: Single, Dual Torch with 101.6 mm (4 in.) gap, Dual Torch with 178 mm (7 in.) gap

Earlier, in these experiments, the torch spacing for the dual torch was fixed at 50.8 mm (2 in.) instead of 101.6 mm (4 in.), to study the effect of torch gap on the weld cooling cycles. However, the plasma interference between the two welding arcs of the torches separated by 50.8 mm (2 in.) caused severe porosity in the weld, which rendered the weld unusable for extracting specimens for small scale testing. After further experimentation, it was evident that to achieve a sound weld deposit, the dual torches had to be at least 101.6 mm (4 in.) apart, in order to negate the interference between the two welding arcs. Serimax, on the other hand, could use a 50.8 mm (2 in.) torch spacing for Third Round of welding due to the proprietary torch design they use for

dual torch welding. All the welds were instrumented with three K-type implantable thermocouples in the HAZ, 12 mm from the bottom of plate similar to second round of pipe welding. As with the pipe welding, all the welds were closely controlled and monitored to record the weld thermal history and weld data, like True Power, Average Heat Input, volts, current, and travel speed. The Lincoln Electric data acquisition system, True Energy™ Meter, was utilized to measure the instantaneous current and voltage data at the rate of 40 KHz. Initial post weld analysis involved conducting 500g Vickers micro-hardness traverses both through the thickness along the weld centerline and in the transverse direction across the weld metal and HAZ at 13.5 mm from the bottom of the plate and correlating it to the variables studied. The detailed results from the flat plate welds are discussed in a separate report 278-T-06 [14].

3.4 Pipe Welds – Third Round

The third round of 5G welding on X100 pipe was completed at two different contractor sites, Contractor A & Contractor B. The results from the statistical analysis of the plate welds showed that the weld composition (P_{cm}), True Heat Input, torch configuration and preheat and interpass temperatures are the major welding variables affecting the hardness, tensile strength, yield strength and Charpy toughness of the weld and HAZ. The variation in P_{cm} was studied by employing X100 pipes from two different sources (A & B, Table 2) and also selecting prototype wires with different P_{cm} , namely PT-1 ($P_{cm}=0.28$) and PT-2 ($P_{cm}= 0.32$) while the effect of torch configuration on weld and HAZ properties was validated using a single and dual torch. It was believed that prototype consumable PT-1 would provide a leaner weld metal in combination with dual torch and hence would not provide the necessary overmatch to the pipe properties. Hence, prototype consumable PT-2, with higher P_{cm} , was used for all dual torch welding in Third Round. Thus, two single torch 5G welds and two dual torch 5G welds were completed on X100 pipes from two sources at each contractor. The minimum preheat and interpass temperatures were maintained very close to 100°C. All the single torch welds were completed using 1.0 mm PT-1 electrode with AWS A5.28M ER76S-G classification while the dual torch welding was completed using 1.0 mm PT-2 electrode with AWS A5.28M ER83S-G classification. The distance between the lead and trail torch for dual torch welding was 120.65 mm (4.75 in.) and 50.8 mm (2 in.) for contractor A & Contractor B respectively. Contractor A utilized their proprietary pulse waveform (GMAW-P) with 85% Ar - 15% CO₂ shielding gas whereas Contractor B utilized the constant voltage process with 50% Ar - 50% CO₂ shielding gas. The detailed information on the torch type, consumable type, welding process and shielding gas used by each contractor is provided in Table 5.

Table 5: Parameters for Third Round Pipe Welding

Pipe Weld #	Contractor	Pipe Type	Torch Type	Wire	Welding Process	Shielding Gas	Preheat / Interpass Temp., °C
952D	A	A	Single	PT-1	GMAW-P	85% Ar-15% CO ₂	100+25-0
952F	A	B	Single	PT-1	GMAW-P	85% Ar-15% CO ₂	100+25-0
952G	A	A	Dual	PT-2	GMAW-P	85% Ar-15% CO ₂	100+25-0
952H	A	B	Dual	PT-2	GMAW-P	85% Ar-15% CO ₂	100+25-0
952I	A	A	Single	PT-1	GMAW-P	85% Ar-15% CO ₂	50+15-0
PRCI-1	B	A	Dual	PT-2	GMAW	50% Ar-50% CO ₂	100+40-0
PRCI-2	B	B	Dual	PT-2	GMAW	50% Ar-50% CO ₂	100+40-0
PRCI-3	B	A	Single	PT-1	GMAW	50% Ar-50% CO ₂	100+40-0
PRCI-4	B	B	Single	PT-1	GMAW	50% Ar-50% CO ₂	100+40-0

As with the previous rounds of welding, all the welds were closely controlled and monitored to record the weld data, like True Power, Average Heat Input, volts, current, and travel speed. A higher sampling frequency of 120 kHz was used for the high speed voltage and current measurements using a True Energy™ meter in an effort to obtain more accurate measure of True Heat Input. However, changing the sampling frequency, from 40 kHz to 120 kHz, did not appear to provide any additional information. Thermocouple plunging in weld puddle of the trail torch using S-type thermocouples was carried out at Contractor B. The intent was to study the effect of narrow (50.8 mm) torch spacing on the weld cooling cycles. The detailed weld chemistry is shown in Table 6 for contractor A welds and Table 7 for contractor B welds. The reported values are averages of the weld chemistries from 12:00, 3:00 and 6:00 o’ clock positions.

Table 6: Weld Metal Chemical Compositions Third Round Pipe Welds at Contractor A using 85%Ar - 15%CO₂ Shielding Gas

Element/Weld	Pipe Type	Torch Type	%C	%Mn	%Si	%Ti	%Cr	%Mo	%Ni	%N	%O	%S	%P	%Al	%Cu
952D	A	ST	0.086	1.64	0.49	0.036	0.17	0.41	1.23	0.004	0.035	0.008	0.015	0.011	0.184
952F	B	ST	0.086	1.65	0.46	0.033	0.29	0.37	1.27	0.005	0.030	0.008	0.014	0.006	0.248
952G	A	DT	0.093	1.62	0.57	0.037	0.22	0.46	1.54	0.004	0.033	0.008	0.013	0.002	0.186
952H	B	DT	0.097	1.69	0.59	0.028	0.37	0.45	1.71	0.004	0.029	0.009	0.010	0.002	0.249
952I	A	ST	0.094	1.60	0.48	0.030	0.17	0.42	1.28	0.004	0.031	0.007	0.015	0.008	0.186

ST – Single Torch , DT – Dual torch

Table 7: Weld Metal Chemical Composition Third Round Pipe Welds at Contractor B using 50%Ar - 50%CO₂ Shielding Gas

Element/ Weld	Pipe Type	Torch Type	%C	%Mn	%Si	%Ti	%Cr	%Mo	%Ni	%N	%O	%S	%P	%Al	%Cu
PRCI#3	A	ST	0.087	1.50	0.46	0.029	0.19	0.44	1.34	0.005	0.047	0.006	0.015	0.003	0.226
PRCI#4	B	ST	0.091	1.52	0.45	0.028	0.26	0.42	1.39	0.004	0.051	0.007	0.014	0.001	0.390
PRCI#1	A	DT	0.094	1.60	0.61	0.024	0.40	0.48	1.92	0.005	0.042	0.010	0.009	0.002	0.232
PRCI#2	B	DT	0.093	1.62	0.66	0.027	0.31	0.51	1.95	0.004	0.040	0.010	0.009	0.004	0.212

ST – Single Torch, DT – Dual Torch

In general, it is evident from the two tables that the weld metal chemical composition (esp. %C, %Mn, %Ti, %Si) from Contractor B is a little leaner than that from Contractor A which is a direct consequence of the higher CO₂ content of the shielding gas used. There is also an obvious difference in the weld metal chemical composition with the single torch (ST) and dual torch (DT), with dual torch chemical composition being slightly richer, due to the higher Pcm wire used for dual torch welding.

The failure to get any meaningful thermal data from the two dual torch 5G pipe welds at Contractor B necessitated a second attempt. An additional dual torch 5G weld was completed simply to acquire thermal data. S-type thermocouples were plunged in the weld puddle of the trail torch between 4:00 and 4:30 position.

Results indicate that the True Heat Inputs were 18-22% higher than the corresponding Average Heat Inputs for the welds made at Contractor A, while there was no appreciable difference between the Average Heat Input and True Heat Input for the welds made at Contractor B. This is reflective of the fact that Contractor A used a pulse waveform while Contractor B used a constant voltage process, highlighting the importance of recording the True Power to get an accurate measurement of heat input into the weld.

3.5 Weld Monitoring - Measurement of Electrical Parameters

Accurate development of the thermal and microstructural models along with proper identification of essential variables requires an equally accurate set of input parameters. The input parameters ranging from dimensional characteristics, chemical composition, temperature cycles, and the welding process all play a role in the complex interactions that ultimately create the properties of a completed weldment.

From an electrical measurement point of view, the welding process is defined by the voltage and amperage. A long list of parameters such as the welding consumable type, shielding gas, wire feed speed, travel speed, contact tip to work distance (CTWD), joint configuration, and welding position all play a role in defining the voltage and amperage but the measurement of these two parameters is largely used to monitor and control the overall process. Therefore, a critical analysis of the measurement systems used on the voltage and amperage is needed to accurately develop and validate the models mentioned above.

Welding processes are generally characterized as constant voltage (CV) or constant current (CC) but both categories are monitored by the measurement of both voltage and amperage. When determining the net effect of the welding process, in terms of thermal characteristics, the measurement of voltage and amperage is used to determine the heat input. As shown in Equation 3, the heat input to the weldment is controlled by voltage, amperage, travel speed, and thermal efficiency of the welding process. For the scope of this work, and some welding specifications, the thermal efficiency is assumed to be constant within a defined set of essential variables and is therefore dropped from the calculation. Equation 4 does not include the thermal efficiency and is widely used for the calculation of heat input [1]; this is named the “Average Heat Input” throughout this topical report.

$$Heat\ Input = \frac{Voltage * Amperage * 60}{Travel\ Speed} * Thermal\ Efficiency$$

[Units: Heat Input = J/in. (or J/mm), Voltage = V, Amperage = A, Travel Speed = in./min (or mm/min), Thermal Efficiency is a unit less percentage]

Equation 3: Average Heat Input with Thermal Efficiency

$$Heat\ Input = \frac{Voltage * Amperage * 60}{Travel\ Speed}$$

Equation 4(a): Average Heat Input

$$Heat\ Input = (Voltage * Amperage) * \left(\frac{60}{Travel\ Speed} \right)$$

Equation 4(b): Components of Average Heat Input

The Average Heat Input calculation is used to define standard welding procedures and can be found in nearly any welding handbook. It provides a mechanism for measuring the heat input into a weldment and is a key parameter for monitoring quality control and consistency. The correlation between heat input, cooling rate and affects on mechanical properties are well known in the welding community and when the essential variables of a welding procedure are maintained within predetermined limits, consistent mechanical properties can be achieved.

The main components of the Average Heat Input calculation, as shown in Equation 4(b), are the power of the welding process (Voltage * Amperage) and a conversion factor along with the travel speed. The exact definition of this “power” and conditions that change its meaning will be discussed in detail; for now, the name used for this quantity will be the “Average Power”. As shown with Equations 3 and 4, the heat input is directly related to the power of the welding process; the following discussions will focus on power measurement and calculation methods. The end result on heat input is a direct relationship.

The Average Heat Input is a reliable indicator that identifies a change in the welding process and the resulting mechanical properties. While the Average Heat Input calculation is a precise measurement within the scope of defined essential variables, it may not provide an accurate measurement of the True Heat Input for all welding processes. This is the classic difference between precise or self-consistent results, and accuracy.

Measurement Precision: The precision of a measurement system is the degree of closeness between replicate measurements on the same or similar objects under specified conditions [2].

Measurement Accuracy: The accuracy of a measurement system is the degree of closeness between a measured quantity value and the true quantity value [2].

In a welding process that has constant direct current (DC) voltage and constant DC amperage, the Average Heat Input calculation is both precise and accurate. In this context, “constant DC” means “similar to DC” with no significant changes over time (the voltage or current is not a periodic time-varying function and there are no significant asymmetric fluctuations from the average value). Examples of welding processes that generally fit into this category are DC gas tungsten arc welding (GTAW), shielded metal arc welding (SMAW), and gas metal arc welding (GMAW) with short circuiting, globular, or spray transfer. Again in this context, the natural inductive response characteristics that are produced with short circuiting or globular transfer processes can be considered “constant DC”. As shown in the following example, the changes in current with these processes are generally symmetric about the average value and do not create a significant accuracy problem. However, a measure of what is “significant”, in terms of changes to the voltage and amperage, can be answered by the manufacturer of the welding power source or determined as explained below.

3.5.1 GMAW Example

Figure 20 shows the voltage and amperage collected from the Lincoln Electric Data Acquisition system during a Third Round Serimax weld and Table 8 lists parameters for the time period between the cursors in this figure. The average value is the arithmetic mean of the voltage or amperage signal (see Equation 5) and the RMS value is the Root Mean Square of the voltage or amperage signal (see Equation 6). The RMS measurement of any signal, constant DC or time-varying, gives the true effective value for calculating power; this true effective value used for calculating power is the equivalent value for an absolutely constant signal. In the case of a constant DC or non time-varying signal, the average and RMS values are equal. In the case of the voltage and amperage signals in Figure 20, there are some time-varying features and the true effective values of the signals are represented by the RMS values. The time-varying features are small (not significant) as can be seen by the percent difference between the average and RMS values. This short circuiting GMAW welding process can be characterized as having constant DC voltage and constant DC amperage; use of the Average Heat Input calculation will produce a result that is both precise and accurate. Before the invention of GMAW-P, or more generally Waveform Controlled Welding, welding processes matched this type of characterization and use of the Average Heat Input calculation provided precise and accurate results without further consideration.

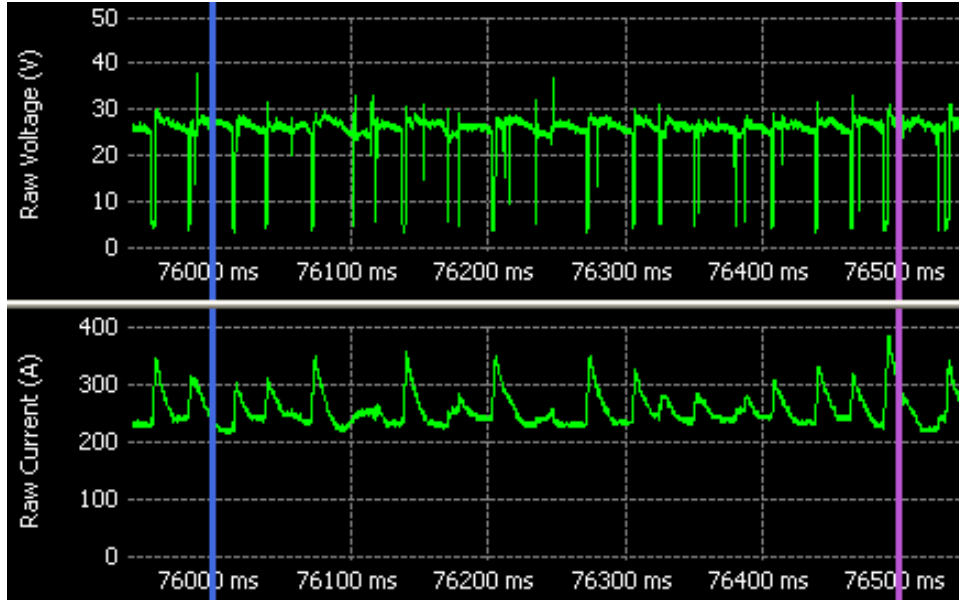


Figure 20: Data from Third Round Weld at Contractor B (Pipe 1 Side 2, Fill Pass 1)

Table 8: Measured Parameters for Figure 20

	Average Value	RMS Value	DC Average Power	True Power	Percent Difference (From RMS or True)
Voltage	25.25 V _{AVG}	25.80 V _{RMS}			-2.13%
Amperage	252.65 A _{AVG}	254.21 A _{RMS}			-0.61%
			6379.41 VA	6384.02 W	-0.07%

$$X_{AVG} = \frac{1}{n} \sum_{i=1}^n x_i$$

Equation 5: Arithmetic Mean (n = number of samples)

$$X_{RMS} = \sqrt{\frac{x_1^2 + x_2^2 + \dots + x_n^2}{n}}$$

Equation 6: Root Mean Square (RMS) (n = number of samples)

3.5.2 GMAW-P Welding Example

In comparison, GMAW-P or Waveform Controlled Welding processes, do not have constant DC voltage or constant DC amperage. ASME Section IX defines Waveform Controlled Welding as: A welding process modification of the voltage and/or current wave shape to control characteristics such as droplet shape, penetration, wetting, bead shape or transfer mode(s) [1]. The power source control and modification of voltage and/or current create time-varying signals that influence the accuracy of the Average Heat Input calculation. While this change in accuracy creates several difficulties when comparing welding processes, the precision of the Average Heat Input calculation is maintained when operating within the scope of defined essential variables.

This means that the Average Heat Input calculation, when used on Waveform Controlled Welding processes, is precise but not accurate. This precision still provides a mechanism for measuring the heat input for monitoring quality control and consistency but the lack of accuracy creates difficulties when comparing the effects of different welding processes and welding waveforms.

Figure 21 shows the voltage and amperage collected from the Lincoln Electric Data Acquisition system during a Third Round CRC weld and Table 9 lists parameters for the time period between the cursors in this figure. Like the previous example, the average and RMS values are calculated with Equations 5 and 6. This GMAW-P welding process has significant changes over time; both the voltage and amperage are time-varying signals. The amperage changes from a peak current of 460 A to a background current of 70 A at a frequency of 160 Hz. The significance of these changes can be seen when comparing the average values and the RMS values in Table 9. The RMS values represent the true effective values for calculating power; the equivalent value for an absolutely constant signal. The average values are correct arithmetic mean values but they do not represent the true effective value for calculating power of a time-varying signal. The difference between average and RMS voltage is -3.24%, possibly not yet significant, but the -21.76% difference between the average and RMS amperage is definitely significant.

Compared to the large difference between the amperage values (-21.76%), the relatively small difference between the voltage values (-3.24%) may seem inconsistent but this is expected. Numerous models for the macroscopic voltage of gas metal arc welding (GMAW) processes can be found with various levels of detail but they all generally have the form shown in Equation 7 [17]. The coefficients k_1 , k_2 , and k_3 are dependent on various parameters such as material type and shielding gas with k_1 and k_2I producing the most dominate characteristics. The magnitude of k_2 is generally near 0.05 so it can be seen that a large change in amperage will only produce a small change in voltage. The amperage fluctuation from peak to background creates a large difference between the average and RMS values. However, these changes in amperage result in only a small voltage fluctuation; the smaller voltage fluctuations produce a smaller difference between the average and RMS values.

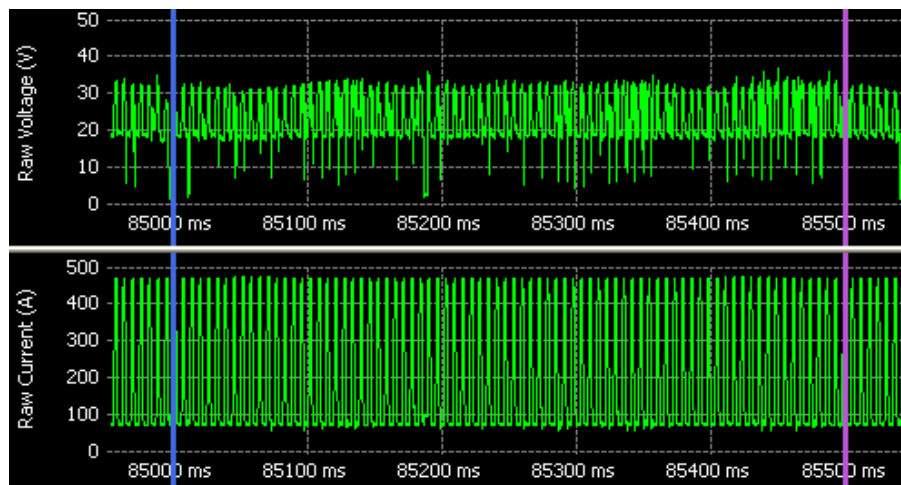


Figure 21: Data from Third Round Weld at Contractor A (952-D Side 1, Fill Pass 1)

Table 9: Measured Parameters for Figure 21

	Average Value	RMS Value	DC Average Power	True Power	Percent Difference (From RMS or True)
Voltage	23.23 V _{AVG}	24.01 V _{RMS}			-3.24%
Amperage	201.15 A _{AVG}	257.11 A _{RMS}			-21.76%
			4672.71 VA	5505.75 W	-15.13%

$$V = k_1 + k_2 I + f(k_3, l_a)$$

[V = Voltage, I = Amperage, l_a = Arc Length]

Equation 7: Macroscopic Voltage of Gas Metal Arc Welding (GMAW) Processes

For this GMAW-P welding process, the Average Heat Input calculation using the average voltage and average amperage values would produce a precise and self-consistent result within the scope of defined essential variables but it has an accuracy error of -15.13%. The True Heat Input for this welding process is 15.13% higher than the result from the Average Heat Input calculation.

3.5.2.1 Average Power and True Power

In order to explain the accuracy error of the previous example, the strict definitions of power and various calculation methods must be discussed. A major component of the Average Heat Input calculation is the power of the welding process (Voltage * Amperage) as shown in Equation 4(b). This calculation method became popular when welding processes could simply be characterized as having constant DC voltage and constant DC amperage. The specific method for measuring the “Voltage” and “Amperage” was not highlighted because the processes were all constant in nature. The standard practice for DC welding equipment, which is still in place today, is to display the average voltage (V_{AVG}) and the average amperage (A_{AVG}) on any metering devices [3]. The loosely defined “Voltage” and “Amperage” used in the Average Heat Input calculation is correctly labeled as the average voltage and average amperage of the welding process. This along with the average travel speed produces the completely defined DC Average Heat Input calculation as shown in Equation 8.

$$Heat\ Input_{AVG} = (Voltage_{AVG} * Amperage_{AVG}) * \left(\frac{60}{Travel\ Speed_{AVG}} \right)$$

Equation 8: DC Average Heat Input

AC (Alternating Current) welding processes are outside the scope of this topical report but the standard practice for AC welding equipment is to display RMS values on any metering devices and the completely defined AC Average Heat Input calculation is shown in Equation 9. Equations 8 and 9 are simply the fully labeled versions of the standard Average Heat Input calculation.

$$Heat\ Input_{AVG} = (Voltage_{RMS} * Amperage_{RMS}) * \left(\frac{60}{Travel\ Speed_{AVG}} \right)$$

Equation 9: AC Average Heat Input

The power of the welding process used in Equation 4(b) and fully labeled in Equation 8 is now understood to be the calculation shown in Equation 10. The resulting DC Average Power of this calculation is only accurate when the average voltage and average amperage values come from constant DC signals. The welding voltage and amperage signals are never perfectly constant DC signals but the significance of the fluctuations (time-varying components) can be minor as in the GMAW welding example. However, as shown with the GMAW-P welding example, the average values of time-varying signals do not represent the true effective value for calculating power. Inaccurate results will be produced from Equation 10 if average values from a time-varying signal are used.

$$Average\ Power = Voltage_{AVG} * Amperage_{AVG}$$

Equation 10: DC Average Power; accurate for constant DC signals only.

The DC Average Power from Equation 10 is listed in Table 8 and 9. The units of these parameters are shown as Volt-Amps (VA) not the normal Watt (W) units for power. This is done in accordance with the correctly labeled units of the equation. Using Watt (W) units would be misleading and it would only be accurate for constant DC signals; in strict electrical engineering terms, this is called Apparent Power and the correct units are Volt-Amps (VA).

The correct method for calculating the True Power with time-varying signals is shown in Equation 11 [3]. This method must be used on time-varying signals to get an accurate result; but, it can be used on any signal type including constant DC signals. Voltage and amperage values are still multiplied together as in Equation 10 but there is a significant difference to be noted. This equation calculates the instantaneous power of every data sample and then takes the average while Equation 10 takes the average of the data samples and then multiplies them together. Equation 10 is the “product of averages” while Equation 11 is the “average of instantaneous power”. The True Power results from Equation 11 are also listed in Table 8 and 9; the units of measure are Watts (W).

$$True\ Power = \frac{1}{n} \sum_{i=1}^n (v_i * i_i)$$

Equation 11: True Power; accurate for any signal type.

The GMAW example in Table 8 was described as “constant DC” because the voltage and amperage signals did not have any significant time-varying components (the difference between the average and RMS is small). This means the Average Power calculation will be accurate as seen by the comparison to the True Power and an error of only -0.07%. The GMAW-P example in Table 9 has time-varying voltage and amperage signals as indicated by the difference between the average and RMS values. The Average Power calculation will be inaccurate; in this case the accuracy error is -15.13%.

3.5.2.2 Average Heat Input and True Heat Input

It was mentioned earlier that the power of the welding process has a direct relationship on the heat input of a welding process. If the Average Power calculation is inaccurate, the resulting heat input calculation will be inaccurate by the same amount. In the GMAW example of Table 8, the Average Power and Average Heat Input has been shown to be accurate and precise. In the GMAW-P example of Table 9, the Average Power and Average Heat Input do not accurately represent the True Power and True Heat Input; the Average Power and Average Heat Input are inaccurate but still precise.

While the Average Heat Input for some welding processes is not accurate, it is repeatable for the purposes of monitoring quality control and consistency. The degree of Average Heat Input inaccuracy is dependent on the specific waveform used for the Waveform Controlled Welding process. Different welding power sources or different types of GMAW-P waveforms can produce accuracy error from 10% to 20%. The Waveform Controlled Welding processes used in this topical report were generally in the range of 8% to 22% as shown in the Topical Report 278-T-06 [14]. However, the degree of inaccuracy is not a fixed amount; different welding power sources and/or different welding waveforms will produce different amounts of error. It is not possible to make precise statements about the degree of accuracy or “offset” for a category of welding processes. When a higher order of accuracy or correlation to cooling rates is required, the True Heat Input must be used.

The list of essential variables for a welding process has been defined for monitoring quality control and consistency but the list does not include every conceivable variable of the process. For example, the list of essential variables does not normally include the exact make and model of the welding power source or an exact waveform definition. It includes the variables that have the most influence on the welding process and, to some degree, the variables that are practical for measurement in a production environment. Use of Average Heat Input, especially for constant DC processes, has served this purpose but the introduction of Waveform Controlled Welding processes and the need for increased process control requires the use of True Heat Input. Use of True Heat Input puts focus on the actual parameter that influences the cooling rate of a weldment; by comparison, complicated waveform definitions could be created but that would only indirectly limit the operation of a power source. Accurately measuring the parameter that influences the process is the best solution for the production environment.

These measurement methods have been used for this project but they are not entirely new concepts as the need for increased heat input accuracy has also lead to recent changes in welding specifications; the 2010 edition of the ASME Boiler and Pressure Vessel Code Section IX is a good example [1]. This welding code now includes the following equations for heat input (True Heat Input) which are based on True Power measured in Watts (W) or True Energy measured in Joules (J). One Joule is equal to one Watt per Second ($1 \text{ J} = 1 \text{ W/s}$). The True Power originates from the instantaneous power calculation stated earlier in Equation 11. True Energy is found by multiplying the True Power by the arc time as shown in Equation 13. Both heat input calculation methods shown in Equation 12(a) and 12(b) produce the same result but one method may be easier to obtain than the other based on the equipment available.

$$\text{True Heat Input}_{AVG} = \frac{\text{True Power} * \text{Arc Time}}{\text{Weld Bead Length}}$$

[Units: Heat Input = J/in (or J/mm), True Power = W,
Arc Time = s, Weld Bead Length = in. (or mm)]

Equation 12(a): Heat input calculated from instantaneous power measurements (see ASME Section IX, QW-409.1(c)); additional notation added for clarity.

$$\text{True Heat Input}_{AVG} = \frac{\text{True Energy}}{\text{Weld Bead Length}}$$

[Units: Heat Input = J/in (or J/mm), True Energy = J,
Weld Bead Length = in. (or mm)]

Equation 12(b): Heat input calculated from instantaneous energy measurements (see ASME Section IX, QW-409.1(c)); additional notation added for clarity.

$$\text{True Energy} = \frac{1}{n} \sum_{i=1}^n (v_i * i_i * t_i) \quad \text{or} \quad \text{True Energy} = \left(\frac{1}{n} \sum_{i=1}^n (v_i * i_i) \right) * \text{Arc Time}$$

Equation 13: True Energy; accurate for any signal type.

Additionally, these measurement methods are also practical for production line pipe welding because some welding power supplies have embedded these measurement methods and meters on the equipment can display True Energy or True Power. These new features not only increase accuracy due to the heat input calculation method but also eliminate another source of error – reading the displayed values of voltage and amperage. The Average Heat Input method would normally require an operator to read and record the displayed voltage and amperage as the values are fluctuating during the welding operation. These values are a source of error because they are an estimated average and the Average Heat Input is then calculated from them. A True Power display, or especially a True Energy display, on an advanced welding power supply eliminates this source of error.

4 CONCLUSIONS & RECOMMENDATIONS

It was evident from the pipe data obtained that that the welding position, 1G or 5G, had little or no effect for achieving a sound and consistent weld throughout the circumference of the pipe as long as the essential welding variables were properly controlled. Thus, proper control of welding variables, especially travel speed, voltage and current, is necessary to minimize the True Heat Input variation of each pass in a multi-pass weld as these have direct correlation to the weld performance and reducing the overall variation in mechanical properties, as demonstrated in Third Round of pipe welding.

Although the success rate for getting relevant thermal data from the HAZ thermocouples was low, the data generated was very useful in furthering the development of numerical thermal models [15]. Some of the challenges encountered were:

- Accurate placement of thermocouples,
- Time and labor involved in making the thermocouples,
- Pre-drilling the holes in the pipe, and
- Spot welding the thermocouples to the base of the drilled holes,
- Consumption of thermocouples due to the high temperature of the welding arc

Most of the S-type thermocouples used to measure the weld thermal profiles were not able to survive the high temperature of the molten weld metal and did not record relevant data. Thermocouple plunging was also challenging for the dual torch welding when the torch spacing was very narrow.

The difference between the True Heat Input measured using a True Energy™ Meter and the calculated Average Heat Input is on average 15-20% for the GMAW-P waveforms used in this investigation, while the difference is negligible in case of constant voltage GMAW. In general, the Average Heat Input, which uses the product of average voltage and current measurements, provides a precise and accurate measurement for constant DC processes such as DC GTAW, SMAW and short circuiting or globular transfer or spray GMAW processes. Average Heat Input is, thus, a reliable indicator that identifies a change in welding process and resulting mechanical properties for non-Waveform Controlled Welding Process mentioned above.

However, for a GMAW-P or Waveform Controlled Welding Process, the Average Heat Input calculation is only capable of producing precise and self-consistent results within the scope of defined essential variables but fails, in terms of accuracy, due to the modification of the voltage and/or current wave shape which creates time-varying signals that influence the accuracy of the Average Heat Input calculations. This change in accuracy is consistent for Average Heat Input as long as the same welding power source and exact same waveform are employed. In comparison, the True Heat Input represents the composite of every instantaneous voltage and current measurement and renders these measurements independent of the welding power source and the waveform. Thus, use of True Heat Input puts focus on accurate measurements of actual parameters that influences the cooling rate of the weldment and hence has been incorporated in the 2010 edition of the ASME Boiler and Pressure Vessel Code Section IX.

5 REFERENCES

1. ASME Boiler and Pressure Vessel Code Section IX – Welding and Brazing Qualifications Available at: <http://www.asme.org>, 2010.
2. International vocabulary of metrology – Basic and general concepts and associated terms (VIM), JCGM 200:2008, Available at: <http://www.bipm.org>, 2008.
3. Bosworth, M.R., “Effective Heat Input in Pulsed Current Gas Metal Arc Welding with Solid Wire Electrodes”, Supplement to the Welding Journal, May 1991.
4. Hudson, M.G., Blackman, S.A., Hammond, J., Dorling, D.V., “Girth welding of X100 pipeline steels”, Paper IPC2002-27296, Proc. of IPC’02, 4th International Pipeline Conference, Calgary, Alberta, pp. 1-8, 2002
5. Hammond, J., Blackman, S.A., Hudson, M.G., “Challenges of girth welding X100 line pipe for gas pipelines” Proceedings of Pipe Dreamer’s Conference, Yokohama, Japan, pp. 1-25, 2002.
6. Hudson, M.G., “Welding of X100 line pipe”, Ph.D. Thesis, Welding Engineering Research Centre, Cranfield University, 2004.
7. Gianetto, J.A., Bowker, J.T., Dorling, D.V., and Horsley, D.J., “Structure and properties of X80 and X100 pipeline girth welds”, Paper IPC04-0316, Proc. of IPC 2004, 5th International Pipeline Conference, Calgary, Alberta, pp. 1-13, 2004.
8. Rajan, V.B., Chen, Y. and Quintana, M.A. , “A new approach to essentials welding variables in girth welding of high strength pipe steels”, Paper IPC2010-31334, Proc. of IPC 2010, 8th International Pipeline Conference, Calgary, Alberta, pp. 1-8, 2010.
9. Glover, A.G., Horsley, D.J., Dorling, D.V., and Takehara, J., “Construction and Installation of X100 Pipelines”, Paper IPC04-0328, Proc. of IPC 2004, 5th International Pipeline Conference, Calgary, Alberta Conference, Calgary, Alberta, 2004.
10. Horsley, D.J., Taylor, D., Hudson, M.G., and Johnson, J., “X100 Field Welding Experience”, APIA-EPRG-PRCI 18th Biennial Joint Technical Meeting, Canberra, Australia, April 2007.
11. Quintana, M.A., and Hammond, J., “X100 Welding Technology – Past, Present and Future”, Paper IPC2010-31421, Proc. of IPC 2010, 8th International Pipeline Conference, Calgary, Alberta, pp. 1-10, 2010.
12. Gianetto, J.A., Tyson, W.R., Goodall, G.R., Rajan, V.B., Quintana, M.A., and Chen, Y., “Microstructure and Hardness Characterization of Girth Welds”, Final Report 278-T-03 to PHMSA per Agreement # DTPH56-07-000005, September 2011.
13. Gianetto, J.A., Tyson, W.R., Goodall, G.R., Chen, Y., Quintana, M.A., Rajan, V.B., and Chen, Y., “Microstructure and Properties of Simulated Weld Metals”, Final Report 278-T-04 to PHMSA per Agreement # DTPH56-07-000005, September 2011.
14. Rajan, V.B., “Examination of Essential Welding Variables”, Final Report 278-T-06 to PHMSA per Agreement # DTPH56-07-000005, September 2011.
15. Chen, Y., Wang, Y.-Y., Quintana, M.A., Rajan, V.B. and Gianetto, J.A., “Thermal Models for Welding Simulations”, Final Report 278-T-07 to PHMSA per Agreement # DTPH56-07-000005, September 2011.
16. Chen, Y., Wang, Y.-Y., Quintana, M.A., Rajan, V.B. and Gianetto, J.A., “Microstructure Model for Welding Simulations”, Final Report 278-T-08 to PHMSA per Agreement # DTPH56-07-000005, September 2011.

17. Reutzel, E.W., Elneron, C.J., Johnson, J.A., Smartt, H.B., Harmer, T., and Moore, K.L., "Derivation and Calibration of a Gas Metal Arc Welding (GMAW) Dynamic Droplet Model", Trends in Welding Research, pages 377-384, June 1995.

6 APPENDIX 1

PROCEDURE FOR CONNECTING AND SETTING-UP THE TRUE POWER METER AND NI SIGNAL EXPRESS FORDOT-PRCI PROJECT

1. Do the fit-up check on pipe assembly and mark the pipe with fit-up lines for best fit orientation.
2. Finalize the distance where the thermocouples are to be placed in the HAZ.
3. Use the drilling gage to set the depth of the drill. After the drill jig is set, drill holes in the pipe. The holes should be almost the same diameter as the thermocouple/ceramic sleeve. Orient the holes to the top of the pipe. If possible cover them up to prevent spatter during ID root welding.

CONNECTING THE THERMOCOUPLES

1. After the root pass, re-orient the holes to the bottom, inspect holes and insert the thermocouples such that the fused end is in contact with the base of the drilled hole. Use a thermocouple welder (dielectric welder) to weld the fused end of the thermocouple to the base of the hole. Make sure the thermocouples are welded properly and do not come off easily.
2. Connect the thermocouple extension wires to the Isothermal terminal block (GREEN BOX). The terminal block has 3 openings for each thermocouple, positive, negative and S. The positive (red) of thermocouple is to be connected to the negative (-) on terminal block and the negative (yellow) of thermocouple is to be connected to the positive (+) on terminal block.
3. Connect the voltage sensor to the Isothermal terminal block. Connect the red (+) lead from the sensor to the wire feeder and the white (-) lead to the welding ground.
4. Connect the NI chassis to the terminal block. One end of the white ground wire for the terminal block is connected to the NI chassis while the other is connected to the welding ground. The NI chassis should be connected to 110V power source without a ground to help eliminate ground loop current (use a ground “cheater plug”). The NI chassis needs to be connected to the laptop via a USB cable.

CONNECTING THE TRUE POWER METER

1. For Current Feedback, connect from negative stud of power source to current out terminal of power meter box and from the current in of the power meter box, to the ground connection on the table for DC+ welding.
2. For voltage feedback, one of the 2 grey cables from the front of the True Power meter, which is positive, is connected to the feeder and the negative one is connected to the welding ground.
3. The True Power meter is connected, without a ground via a ground cheater plug, to the isolation transformer.
4. Ethernet cable is connected from the True Power meter to the second laptop which has the WeldDAQ software installed.

RECORDING DATA WITH THE TRUE POWER METER

1. Clicks open the WeldDAQ program.
2. For the first time installation, File→ Connect → Select “I do not know the IP address of the welder”. The computer will search for the IP address. Select the IP address put forth by the computer and hit “Connect”. Once the IP address is assigned to the True Power meter, this step does not need to be repeated. The True Power will have to be connected at the start of each shift every day.
3. Check/Select the Raw Voltage and Raw Current fields to record the information during welding.
4. Set the data collection frequency to 40 KHz (40,000 Hz).
5. Make a folder on the laptop hard drive to save the WeldDAQ “wdq” files.
6. Before every pass, manually go in and change the file/pass name. -- VERY IMPORTANT
7. Please make sure to remove the power cord from the laptops during data acquisition to minimize any ground loop interference.

RECORDING DATA WITH THE NI SIGNAL EXPRESS

1. START→ Programs→ Open National Instruments Labview Signal Express. Wait until the program is fully loaded.
2. Menu→ Add Step→ Acquire Signals→DAQMX Acquire→Analog
Input→Voltage Select ai0→ok
Set range for Input Voltage→ +10V to -5V
Terminal Configuration→ Differential
Custom Scaling→ No Scale
3. Click “+” to add channels→ Thermocouple
Select ai1 thru ai9 (or however many thermocouples are being used)→ok
4. Go to “Settings” Tab (For HAZ thermocouples)
Expected Input Range → 1300 max, 20 min deg C
Thermocouple Type → K
CJC Source → Built-In
5. Select ai10 (or the next available ai number) (For Plunge Thermocouple)
Expected Input Range → 1700 max, 20 min deg C
Thermocouple Type → S
CJC Source → Built-In
6. Timing Settings
Acquisition Mode → Continuous samples
Samples to Read → 500
Rate (Hz) → 1K
Menu→ Add Step→ Load/Save Signals→ Analog Signals→ Save to ASCII/LVM
Select “SIGNAL” Tab
Add Input→Select ai0→ Ok
Add Input→Select ai1 → Ok
...
Add Input→Select ai10→ Ok
File Settings Tab
Export File Path→ Browse for path and type in filename
If File already Exists→ Select “Append to File”
Export File Type→ Generic ASCII (.txt)
Delimiter→ Tab
Include Signal Names→ Check mark
X value Columns→ One column per channel
Time Axis Preference→ Absolute time
Press “RUN” to start recording data. Wait for 2-3 minutes after welding is completed to stop recording the data by pressing “STOP”.